

AD-A264 354



# ENTATION PAGE

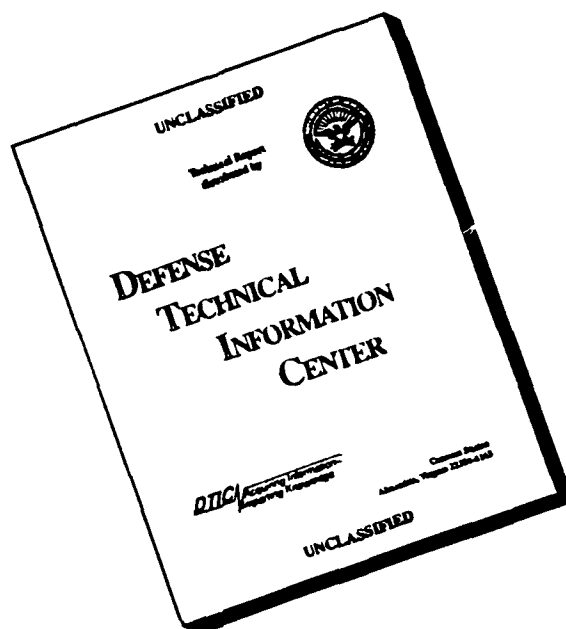
Form Approved  
OMB No. 0704-0188

(2)

THIS REPORT IS THE PROPERTY OF THE U.S. GOVERNMENT. IT IS TO BE DISTRIBUTED TO ALL FEDERAL AGENCIES AND TO THE PUBLIC. IT IS TO BE REPRODUCED AND TRANSMITTED IN ANY FORM AND BY ANY MEANS, ELECTRONIC OR MECHANICAL, INCLUDING PHOTOCOPYING, RECORDING, OR BY ANY INFORMATION STORAGE AND RETRIEVAL SYSTEM, WITHOUT PERMISSION OF THE U.S. GOVERNMENT. THIS REPORT IS THE PROPERTY OF THE U.S. GOVERNMENT. IT IS TO BE DISTRIBUTED TO ALL FEDERAL AGENCIES AND TO THE PUBLIC. IT IS TO BE REPRODUCED AND TRANSMITTED IN ANY FORM AND BY ANY MEANS, ELECTRONIC OR MECHANICAL, INCLUDING PHOTOCOPYING, RECORDING, OR BY ANY INFORMATION STORAGE AND RETRIEVAL SYSTEM, WITHOUT PERMISSION OF THE U.S. GOVERNMENT.

1. AGENCY USE ONLY (Leave blank)		2. REPORT DATE March 1993		3. REPORT TYPE AND DATES COVERED Final Report 3/15/89 -3/14/92	
4. TITLE AND SUBTITLE Structural Development in Ceramic Precursor Sols and Gels				5. FUNDING NUMBERS  61102F 2303 A3	
6. AUTHOR(S) Martha L. Mecartney					
7. PERFORMING ORGANIZATION NAME(S) AND ADDRESS(ES)  Univ of Minnesota, ORTTA 1100 Washington Ave S. Ste 201 Minneapolis, MN 55415-1226				8. PERFORMING ORGANIZATION REPORT NUMBER  AFOSR-TR- 93 0218	
9. SPONSORING / MONITORING AGENCY NAME(S) AND ADDRESS(ES)  AFOSR/NC Building 410, Bolling AFB DC 20332-6448				10. SPONSORING / MONITORING AGENCY REPORT NUMBER  F49620-89-C-0050	
11. SUPPLEMENTARY NOTES					
12a. DISTRIBUTION AVAILABILITY STATEMENT  APPROVED FOR PUBLIC RELEASE; DISTRIBUTION IS UNLIMITED.				12b. DISTRIBUTION CODE	
13. ABSTRACT (Maximum 200 words) See Attached					
<div style="text-align: right;"> OTIC  ELECTE  MAY 14 1993  S B D </div> <div style="text-align: center;"> 93 5 13 03 6 </div> <div style="text-align: right;"> 93-10739  </div>					
14. SUBJECT TERMS				15. NUMBER OF PAGES 48	
				16. PRICE CODE	
17. SECURITY CLASSIFICATION OF REPORT  UNCLASSIFIED		18. SECURITY CLASSIFICATION OF THIS PAGE  UNCLASSIFIED		19. SECURITY CLASSIFICATION OF ABSTRACT  UNCLASSIFIED	
20. LIMITATION OF ABSTRACT					

# DISCLAIMER NOTICE



THIS DOCUMENT IS BEST QUALITY AVAILABLE. THE COPY FURNISHED TO DTIC CONTAINED A SIGNIFICANT NUMBER OF PAGES WHICH DO NOT REPRODUCE LEGIBLY.

13. The effect of water of hydrolysis on nucleation, crystallization, and micro- structural development of sol-gel derived single phase  $\text{LiNbO}_3$  thin films has been studied using transmission electron microscopy (TEM), atomic force micro- scopy (AFM), X-ray diffraction (XRD), and differential scanning calorimetry (DSC). A precursor solution of double ethoxides of lithium and niobium in ethanol was used for the preparation of sol. DSC results indicated that adding water to the solution for hydrolysis of the double ethoxides lowered the crystallization temperature from  $500^\circ\text{C}$  (no water) to  $390^\circ\text{C}$  (2 moles water per mole ethoxide). The amount of water had no effect on the short range order in amorphous  $\text{LiNbO}_3$  gels but rendered significant micro- structural variations for the crystallized films. AFM studies indicated that surface roughness of dip coated films increased with increasing water of hydrolysis. Films on glass, heat treated for 1 hour at  $400^\circ\text{C}$ , were polycrystalline and randomly oriented. Those made with a low water to ethoxide ratio had smaller grains and smaller pores than films prepared from sols with higher water to ethoxide ratios. Annealing films with a low water concentration for longer times or at higher temperatures resulted in grain growth. Higher temperatures ( $600^\circ\text{C}$ ) resulted in grain facetting along close packed planes. Films deposited on c-cut sapphire made with a 1:1 ethoxide to water ratio and heat treated at  $400^\circ\text{C}$  were epitactic with the c-axis perpendicular to the film-substrate interface. Films with higher concentrations of water of hydrolysis on sapphire had a preferred orientation but were polycrystalline. It is postulated that a high amount of water increases the concentration of amorphous  $\text{LiNbO}_3$  building blocks in the sol through hydrolysis, which subsequently promotes crystallization during heat treatment.

Copy available to DDC does not  
permit fully legible reproduction

DTIC QUALITY INSPECTED 8

Accession For	
NTIS GRA&I	<input checked="checked" type="checkbox"/>
DTIC TAB	<input type="checkbox"/>
Unannounced	<input type="checkbox"/>
Justification	
By	
Distribution/	
Availability Codes	
Dist	Avail and/or Special
A-1	

**Final Technical Report****AFOSR Contract # F49620-89-C-0050****"Structural Development in Ceramic Precursor Sols and Gels"**

Principle Investigator, Martha L. Mecartney  
Department of Mechanical & Aerospace Engineering  
University of California, Irvine  
(Originally, Department of Chemical Engineering & Materials Science  
University of Minnesota)

**PUBLICATIONS (copies previously sent except those marked \*\*):**

1. J.K. Bailey and M.L. Mecartney, "Characterization of Structural Development in Sol-Gel Systems by Cryo-TEM," to be published in Proceedings of 4th Ultrastructure Conference (1989), John Wiley & Sons.
2. T. Nagase, "Rheology of Ceramic Sol-Gel Systems During Gelation," M.S. Thesis, Department of Chemical Engineering & Materials Science, University of Minnesota, 1990.
3. "TEM Analyses of Sol-Gel Derived and Sputtered PZT Thin Films," by C.C. Hsueh and M.L. Mecartney, in Ferroelectric Thin Films, Mat. Res. Soc. Symp. Proc. vol. 200, pp. 219-224 (1990).
4. "Vanadium Pentoxide Gels: Structural Development and Rheological Properties," by J.K. Bailey, T. Nagase, G.A. Pozarnsky, and M.L. Mecartney, in Better Ceramics Through Chemistry IV, Mat. Res. Soc. Symp. Proc. vol. 180, pp. 759-764 (1990).
5. "Rheology for Better Sol-Gel Fiber and Film Formation," by C.W. Macosko, M.L. Mecartney, and L.E. Scriven, in Better Ceramics Through Chemistry IV, Mat. Res. Soc. Symp. Proc. vol. 180, pp. 555-568 (1990).
6. "Microstructural Development and Electrical Properties of Sol-Gel Prepared Lead Zirconate-Titanate Thin Films," C.C. Hsueh and M.L. Mecartney, J. Mater. Res. 6 [10] 2208-2217 (1991).
7. "Crystallization Behavior of Chemically Synthesized LiNbO<sub>3</sub>," by Vikram Joshi. Proceedings of the Electron Microscopy Society of America, pp. 964-965 (1991).
8. "Direct Observation and Modeling of Microstructural Development in Chemical Processing of Ceramics," Ph.D. Thesis of Joseph Bailey, University of Minnesota, 1991.

Approved for public release;  
distribution unlimited.

*Let's discuss quantum*

9. "Sol-Gel Processing, Microstructural Development, and Electrical Properties of Ferroelectric Lead Zirconate-Titanate Thin Films," Ph.D. Thesis of Cheng-Chen Hsueh, University of Minnesota, 1991.
10. J.K. Bailey, G.A. Pozarnsky, and M.L. Mecartney, "The Direct Observation of Structural Development During Vanadium Pentoxide Gelation," J. Mater. Res., 7 [9] 2530-2537 (1992).
11. V. Joshi, G. Goo, and M.L. Mecartney, "Microscopy Studies of Sol-Gel Derived Lithium Niobate," in Synthesis and Processing of Ceramics: Scientific Issues, Mat. Res. Soc. Symp. Proc. vol. 249, pp. 459- (1992).
12. C. Hsueh and M. L. Mecartney, "Microstructural Evolution of Sol-Gel Derived PZT Thin Films," Ferroelectric Thin Films, Mat. Res. Soc. Symp. Proc. vol. 243, pp. 451-456 (1992).
- \*\*13. Vikram Joshi, Grace Goo and Martha Mecartney, "Microstructural Variations in Sol-Gel Processed Lithium Niobate Thin Films," Mat. Res. Soc. Symp. Proc. vol. 271, Better Ceramics Through Chemistry, pp. 377-382 (1992).
- \*\*14. Vikram Joshi and Martha L. Mecartney, "The Influence of Water of Hydrolysis on Microstructural Development in Sol-Gel Derived Lithium Niobate Thin Films," submitted for publication.
- \*\*15. Vikram Joshi Ph. D. Thesis, "Lithium Niobate Thin Films via Sol-Gel Processing," in preparation.

#### CONFERENCE PRESENTATIONS:

1. "Characterization of Sol and Gel Structures by Cryo-TEM," First International Ceramic Science and Technology Congress (American Ceramic Society), Anaheim, CA, November 1989.
2. "Structural Development during Sol-Gel Processing," (coauthors J.Bailey and T.Nagase) American Institute of Chemical Engineers Annual Meeting, San Francisco, CA, November 1989.
3. "Microstructural Development during the Sol-Gel Study of Lithium Niobate," (coauthors V. Joshi and J.K. Bailey), MRS Spring Meeting, San Francisco, April 1990.
4. "Rheology for Better Sol-Gel Fiber and Film Formation," (presented by L.E. Scriven, coauthors L.E. Scriven and C.W. Macosko) MRS Spring Meeting, San Francisco, April 1990.
5. "Vanadium Pentoxide Gels: Structural Development and Rheological Properties," (coauthors J.K.Bailey, T. Nagase, G.Pozarnsky) MRS Spring Meeting, San Francisco, April 1990.
6. "TEM Analyses of Sol-Gel Derived and Sputtered PZT Thin Films," (presented by coauthor C.C. Hsueh) MRS Spring Meeting, San Francisco, April 1990.
7. "Formation of Colloidal Silica Particles from Alkoxides," Ralph K. Iler Memorial Symposium, ACS National Meeting, Washington D.C. August 1990 (invited talk, presented by graduate student J. Bailey).

8. "Structural Development During Sol-Gel Processing," Powder Free Processing of Advanced Ceramics Workshop, Schloss Ringberg, Germany (Sponsored by Max Planck Gesellschaft, NATO Scientific Affairs Division, Brussels, Office of Naval Research, London, and NSF) November 1990 (invited talk).
9. "Morphological Characterization of Gel Ultrastructures," Fifth Ultrastructure Processing Conference, Orlando, Florida, February 1990 (invited talk).
10. "Sol-Gel Processing of  $\text{LiNbO}_3$ ," Fifth Ultrastructure Processing Conference, Orlando, Florida, February 1990 (with Vikram Joshi).
11. "Crystallization Behavior of Chemically Synthesized  $\text{LiNbO}_3$ ," Electron Microscopy Society of America Annual Meeting, San Jose, August 1991 (presented by Vikram Joshi).
12. "Microstructural Development in Sol-Gel Processing," AIChE Fall Meeting, Los Angeles, November 1991 (invited talk).
13. "Microscopy Studies of Sol-Gel Derived Lithium Niobate," V. Joshi, G. Goo, and M.L. Mecartney, Synthesis and Processing of Ceramics Symposium Mat. Res. Soc. Fall 1991 Meeting.
14. "Microstructural Evolution of Sol-Gel Derived PZT Thin Films," C. Hsueh and M. L. Mecartney, Ferroelectric Thin Films Symposium, Mat. Res. Soc. Fall 1991 Meeting.
15. "Sol-Gel Derived Lithium Niobate Thin Films," Vikram Joshi, Grace Goo, and Martha Mecartney, Am. Ceramics Society 94th Annual Meeting, Minneapolis, April 1992.
16. "Microstructural Variations in Sol-Gel Processed Lithium Niobate Thin Films," Vikram Joshi, Grace Goo and Martha Mecartney, Better Ceramics Through Chemistry Symposium, Materials Research Society Spring Meeting, 1992.
17. "Substrate Influenced Nucleation and Crystallization of  $\text{LiNbO}_3$  Thin Films Made by Sol-Gel," Vikram Joshi and Martha Mecartney, accepted for presentation at the MRS Spring Meeting 1993, Ferroelectric Thin Films Symposium.
18. "The Role of Hydrolysis in Epitaxial Growth of Sol-Gel Derived  $\text{LiNbO}_3$  Thin Films on Sapphire," Vikram Joshi and Martha Mecartney, accepted for presentation at the MRS Spring Meeting 1993, Ferroelectric Thin Films Symposium.
19. "Process/Property Correlations in Sol-Gel Derived  $\text{LiNbO}_3$  and  $\text{KNbO}_3$  Thin Films," Debassis Roy, Vikram Joshi, Garo Derderian, and Martha Mecartney, accepted for presentation at 5th International Symposium on Integrated Ferroelectrics, Colorado Springs, 1993.

#### INVITED SEMINARS:

1. "Microstructural Evolution and Rheological Behavior During the Gelation of Ceramic Sols" Department of Chemical Engineering, California Institute of Technology, March 1989.
2. "Microstructural Evolution and Rheological Behavior During the Gelation of Ceramic Sols," Department of Chemical Engineering, University of California, Santa Barbara, March 1989.

3. "Microstructural Evolution and Rheological Behavior During the Gelation of Ceramic Sols," Department of Polymer Science, University of Massachusetts, Amherst, March 1989.
4. "Microstructural Evolution and Rheological Properties During the Gelation of Ceramic Sols," Department of Chemical Engineering, Purdue University, April 1989.
5. "Microstructural Studies of Gel Formation Using Cryo-microscopy," TRW, Redondo Beach, California, May 1989.
6. "Microstructural Evolution and Rheological Behavior During the Gelation of Ceramic Sols," Department of Materials Science and Engineering, UCLA, July 1989.
7. "Microstructural Evolution and Rheological Behavior During the Gelation of Ceramic Sols," Department of Chemical Engineering, Washington State University, October 1989.
8. "Structural Evolution During Sol-Gel Processing," Department of Chemical Engineering, University of New Mexico, Albuquerque, January 1990.
9. "Sol-Gel Processing and Structural Development in PZT and  $V_2O_5$  Systems," Sandia National Labs, Albuquerque, January 1990.
10. "Chemical Processing of Ceramics," Chemical Engineering Department, Georgia Tech, Atlanta, GA, May 1990.
11. "Sol-Gel Processing of Ferroelectric Thin Films," Hughes Research Labs, Malibu, CA March 1992.
12. "Sol-Gel Processing of Ceramic Materials," Physical Chemistry Div. Dept. of Chemistry, UCI, April 1992.
13. "Crystallization of Sol-Gel Thin Films," Crystal Growers Association of Southern CA, June 1992.

# The Influence of Water of Hydrolysis on Microstructural Development in Sol-Gel Derived $\text{LiNbO}_3$ Thin Films

Vikram Joshi\* and Martha L. McCartney\*\*

\*Department of Chemical Engineering & Materials Science

University of Minnesota

Minneapolis, MN 55455

\*\*Materials Science & Engineering Program

Department of Mechanical & Aerospace Engineering

University of California

Irvine, CA 92717



## ABSTRACT

The effect of water of hydrolysis on nucleation, crystallization, and microstructural development of sol-gel derived single phase  $\text{LiNbO}_3$  thin films has been studied using transmission electron microscopy (TEM), atomic force microscopy (AFM), X-ray diffraction (XRD), and differential scanning calorimetry (DSC). A precursor solution of double ethoxides of lithium and niobium in ethanol was used for the preparation of sol. DSC results indicated that adding water to the solution for hydrolysis of the double ethoxides lowered the crystallization temperature from  $500^\circ\text{C}$  (no water) to  $390^\circ\text{C}$  (2 moles water per mole ethoxide). The amount of water had no effect on the short range order in amorphous  $\text{LiNbO}_3$  gels but rendered significant microstructural variations for the crystallized films. AFM studies indicated that surface roughness of dip coated films increased with increasing water of hydrolysis. Films on glass, heat treated for 1 hour at  $400^\circ\text{C}$ , were polycrystalline and randomly oriented. Those made with a low water to ethoxide ratio had smaller grains and smaller pores than films prepared from sols with higher water to ethoxide ratios. Annealing films with a low water concentration for longer times or at higher temperatures resulted in grain growth. Higher temperatures ( $600^\circ\text{C}$ ) resulted in grain facetting along close packed planes. Films deposited on c-cut sapphire made with a 1:1 ethoxide to water ratio and heat treated at  $400^\circ\text{C}$  were epitactic with the c-axis perpendicular to the film-substrate interface. Films with higher concentrations of water of hydrolysis on sapphire had a preferred orientation but were polycrystalline. It is postulated that a high amount of water increases the concentration of amorphous  $\text{LiNbO}_3$  building blocks in the sol through hydrolysis, which subsequently promotes crystallization during heat treatment.

## 1. INTRODUCTION

Lithium niobate is an important ferroelectric material due to its unique properties such as a very high spontaneous polarization, a very high Curie temperature (1210°C), and a large negative birefringence [1, 2, 3]. Thin films of  $\text{LiNbO}_3$  are of current research interest because of the demand for active integrated optical devices [4, 5, 6]. Sol-gel processing promises to be a viable process technique for growing  $\text{LiNbO}_3$  films on various substrates as it facilitates lowering the temperature of crystallization and obtaining the correct stoichiometry [7, 8, 9]. Processing parameters such as solution chemistry, deposition technique, firing conditions, and substrate are known to influence the development of film crystallinity, porosity, grain size, and growth morphology during sol-gel processing [10, 11, 12]. It has also been shown that the structure of sol-gel derived  $\text{LiNbO}_3$  thin films sensitively depends on the prior processing [13]. In order to produce optimal film microstructures for practical applications of ferroelectric thin films in electrical and optical systems, the connection between processing and the resultant microstructure is essential. The objective of this work, therefore, was to investigate the effect of specific processing parameters on the microstructural development and crystallization of  $\text{LiNbO}_3$  thin films made from double metal alkoxide solutions.

In particular, the water of hydrolysis was considered critical to investigate with respect to its effect on the nucleation and crystallization process and the consequent microstructural development of the  $\text{LiNbO}_3$  phase from the amorphous gel. Water is deliberately added to promote hydrolysis and condensation but water is present also in the atmosphere and is a by-product of hydrolysis and condensation. Much of the research on water concentration effects on sol-gel derived ferroelectric thin films has focused on X-ray diffraction (XRD) studies of crystallization and phase development with little attention to microstructural details [9,12]. Hirano and Kato [14] have shown that heat treatment of sol-gel derived  $\text{LiNbO}_3$  thin films in an atmosphere of water vapor and  $\text{O}_2$  helps in lowering the crystallization temperature. XRD studies by Nashimoto and Cima [9] reported increased orientation of  $\text{LiNbO}_3$  films on sapphire with reduced water levels in the sol, unhydrolyzed sol yielding epitaxial films. These studies indicate a significant role for

water in crystallization, but it is not yet understood how the degree of hydrolysis controls microstructural development is critical.

A second parameter chosen to investigate was the relationship between the choice of substrate and the crystallization behavior. Amorphous silicate glass substrates were chosen in order to study nucleation and grain morphology in polycrystalline  $\text{LiNbO}_3$  films. Thin films were also deposited on c-cut sapphire substrates for epitaxial crystallization. These latter substrates should promote optimal orientation for certain device applications. Bulk gels, unconstrained by substrates, were also studied to compare their nucleation and crystallization behavior with thin films.

## II. EXPERIMENTAL

Based on the method outlined by Hirano and Kato [14], a 0.5 molar stock solution of double metal ethoxide was prepared by refluxing lithium and niobium ethoxide in ethanol for 24 hours. Small portions of the stock solution were partially hydrolyzed by using an ethanol-water mixture to induce gelation. Three different water concentrations were used for hydrolysis, 1, 2, and 3 moles of water for each mole of ethoxide. The obtained gels were air dried at room temperature and were characterized by transmission electron microscopy (TEM) and differential scanning calorimetry (DSC). DSC was performed in air for partially hydrolyzed gels and in both air and nitrogen for unhydrolyzed powders at heating rates of  $10^\circ\text{C}/\text{min}$ .

Spinnable solutions of 0.25 molarity were prepared by dilution of the stock solution with an ethanol-water mixture. Sols with no water, 1:1, and 1:2 ethoxide to water ratio were prepared. Sols having ethoxide to water ratio of 1:3 showed such a rapid increase in viscosity and quick gelation so that no films could be spun. Microscope glass slides and c-cut sapphire (Insaco inc., Quakertown, PA) were cleaned ultrasonically in acetone, 20% HCl solution, and de-ionized water in that order. The substrates were heat treated up to  $350^\circ\text{C}$  for 15 min., then cooled down to room temperature right before the coating was started in order to decompose any residual on the surface of the substrate.

Glass substrates were dip coated in the precursor solution and were withdrawn at a speed of 5 cm/min.. Sapphire substrates were spin-coated at 2000 rpm. Each coating layer was dried at 300°C on a hot plate for 1 min. and produced a film thickness of about 60 nm for dip coating and 40 nm for spin coating. The coating and heating steps were repeated as many times as necessary to achieve a desired thickness. As-deposited  $\text{LiNbO}_3$  thin films were then heated to temperatures from 400°C to 600°C at a ramp rate of 10°C/min in an air ambient, maintained at the annealing temperature for times from 1 to 4 hours, and then furnace cooled.

Microstructural characterization of the films was primarily accomplished by TEM. Specimens for TEM analysis were prepared using standard specimen preparation techniques for cutting, polishing, dimpling, and ion milling. Cryo-TEM samples were prepared according to the technique described by Bailey et al [15]. TEM work was carried out on JEOL 100CX, Philips CM30, and Philips CM20 transmission electron microscopes. A double tilt cold stage cooled with liquid nitrogen was used in order to reduce electron beam heating effects. The use of plan-view geometries enabled observation of the film microstructure while obtaining electron diffraction information about the in-plane orientation of the film.

### III. RESULTS

#### A. Microstructure of wet and dried films

Figure 1 shows the cryogenic transmission electron micrograph and corresponding selected area diffraction (SAD) pattern of the frozen sol with an ethoxide to water ratio of 1:2 at 75% of the gelation time. A rather featureless microstructure and a diffuse halo in the SAD pattern are observed. No phase separation or precipitate formation in this partially hydrolyzed sol is observed.

TEM micrographs of films of lithium niobium ethoxide sols deposited on carbon coated formvar TEM support grids are shown in Figure 2. These micrographs give the first indication of variations between different ethoxide to water ratios. An increase in the amount of water of hydrolysis results in an increased pore size for these thin film gels. The film deposited from

unhydrolyzed sol is of uniform thickness and very dense. Pores on the order of 5 nm or less are visible in the 1:1 film, whereas, the 1:2 film is even coarser with pore size varying between 2-10 nm. Diffuse halos in the SAD patterns were analyzed for short range order in these amorphous films. The interatomic distance corresponding to the maximum intensity of the first and second strongest halos are 3.7 Å and 2.0 Å respectively for all samples, even with differing amount of water.

### **B. Thermal analysis**

The crystallization kinetics of the amorphous gels was studied by DSC. Figure 3 shows DSC traces from 200 to 600°C for gels formed under different hydrolysis conditions. Below this temperature range, all compositions had an endothermic peak at about 100°C, associated with the removal of residual solvent and water. Exothermic transformations are observed in the 200 to 600°C region. The exothermic peak around 325°C is associated with a weight loss as observed by TGA. This weight loss, which could be interpreted as corresponding to the decomposition of bound organic species, precedes an exothermic transformation at temperatures near 400°C which represents crystallization of amorphous  $\text{LiNbO}_3$  (as confirmed by the XRD results). The exothermic peak temperatures are at 390 and 410°C for the 1:2 and 1:1 gels respectively. Unhydrolyzed powders crystallized at 500°C when heated in a nitrogen atmosphere but in air, these powders showed two exotherms, at 400 and 500°C. The two exotherms were most likely due to the fact that the highly reactive powder surfaces were probably partially hydrolyzed when heated in air and so the two peaks would correspond to the crystallization of hydrolyzed and unhydrolyzed regions.

### **C. Nucleation and crystallization in $\text{LiNbO}_3$ powders and gels**

Phase formation and microstructural changes during the amorphous to crystalline transformation in 1:2 dried gel were observed in the transmission electron microscope. When a sample was heated to 200°C very fine crystallites of  $\text{LiNbO}_3$  of a size less than 20 nm nucleated in

an amorphous matrix within 30 min. (Fig. 4a). The electron diffraction pattern of this area shows the appearance of distinct spots along with the presence of diffuse rings, indicating the onset of crystallization. The powders were further heated at a rate of  $10^{\circ}\text{C}/\text{min}$  and were held at  $400^{\circ}\text{C}$  for 30 min. At  $450^{\circ}\text{C}$ , in certain samples spherical particles were formed (Fig. 4b). These crystalline particles range in size from approximately 50-200 nm. At  $600^{\circ}\text{C}$ , large crystallites on the order of  $1\text{ }\mu\text{m}$  are observed (Fig. 4c). The SAD pattern from one such particle is essentially that of a single crystal. The side facet faces are the first order prism planes,  $\{10\bar{1}0\}$  and the top and bottom faces are basal planes  $(0001)$  (normal to the zone axis  $[0001]$ ).

#### D. Thin films on amorphous substrates

Atomic force microscopy (AFM) is a very useful technique for monitoring the surface topology of non-conducting surfaces [16]. AFM of  $\text{LiNbO}_3$  thin films on glass was used to determine the effects of the amount of water of hydrolysis on surface roughness of films on glass (heat treated at  $400^{\circ}\text{C}$ ). One can see in Figure 5 that the dip coated  $\text{LiNbO}_3$  thin films after heat treatment at  $400^{\circ}\text{C}$  for 1 hour show increased surface roughness (on the order of 10 nm) as the ethoxide to water ratio changed from 1:1 to 1:2. Films deposited from unhydrolyzed (1:0) and 1:1 sols were extremely smooth (on the order of 2 nm).

Crystallization as a function of water of hydrolysis in  $1200\text{\AA}$  thick  $\text{LiNbO}_3/\text{glass}$  films was studied by TEM analysis. Figure 6 shows TEM micrographs of  $\text{LiNbO}_3$  films on glass fired at  $400^{\circ}\text{C}$  for 1 hour. The film deposited on glass using an unhydrolyzed sol was amorphous at  $400^{\circ}\text{C}$  (Fig. 6a), but the films made with partially hydrolyzed sols crystallized at  $400^{\circ}\text{C}$  (Figures 6b and 6c). The 1:1 film appears relatively dense with a grain size in the range of 20-30 nm. The selected area diffraction (SAD) pattern indicates the polycrystalline nature of the film. The rings in the SAD pattern index to the  $d$  spacings of the  $\text{LiNbO}_3$  crystal structure. A very different microstructure was observed for 1:2 film. Distinctive microstructural features of this film are large pores and a large grain size on the order of 150 nm. The pore and the grain size are of similar size and the pores appear as holes in the 120 nm thick film (Fig. 6c).

The influence of annealing temperature in 1:1 film microstructure is shown in Figure 7a. With heat treatments, the average crystallite size in the film increased from 30 nm at 400°C to 125 nm at 600°C for 1 hour. More diffraction rings are observed in the SAD pattern of this film compared to the films heat treated at 400°C for 1 hour. The excess rings indexed to the Li deficient phase  $\text{LiNb}_3\text{O}_8$ .

Figure 7b shows the microstructure of 1:1  $\text{LiNbO}_3$  film on glass substrate annealed at 400°C for 4 hour. Compared to Figure 7a (600°C, 1 hour), these longer heat treatment times result in grain growth but no development of any second phase. SAD pattern of this film confirmed the presence of single phase  $\text{LiNbO}_3$ . After 4 hour of soaking time, the average grain size in the 1:1 film was on the order of 150 nm, similar to the grain size observed in 1:2 film, annealed at 400°C for 1 hour. However, the 1:1 film at 400°C for 4 hours remained relatively dense and free of large pores, unlike the microstructure of 1:2 film at 400°C for 1 hour.

#### E. Thin films on (0001) sapphire substrates

$\text{LiNbO}_3$  thin films on (0001) sapphire were also examined by TEM and XRD. Figures 8 and 9 show regions of a film spun coated using a sol with  $\text{LiNb}(\text{OC}_2\text{H}_5)_6:\text{H}_2\text{O}$  ratio of 1:1 and annealed at 400°C for 1 hour. The underlying substrate was completely removed during ion milling. Figure 8 shows a typical bright-field and dark-field image of a  $\text{LiNbO}_3$  thin film on (0001)-oriented sapphire. The prominent features of this film are its single crystal nature and absence of porosity. The sharp diffraction spots of the [0001] zone axis in Figure 8a indicate growth well oriented with respect to the substrate. However, Figure 9 shows another area of this film, where twinning along the  $[10\bar{1}0]$  direction is observed. Thickness fringes and dislocations are also noticeable in the images shown in Figures 8 and 9.

Figure 10a is a high magnification image of a region where the film was still attached to the substrate. Moiré fringes are observed in this micrograph. Figure 10b shows the corresponding SAD pattern taken with the electron beam parallel to the sapphire [0001] zone axis. This SAD

pattern demonstrated that the  $\text{LiNbO}_3$  thin film was epitaxially grown onto the sapphire substrate with the following orientation relationship:

$$(0001) \text{LiNbO}_3 // (0001) \text{ sapphire and } [11\bar{2}0] \text{LiNbO}_3 // [11\bar{2}0] \text{ sapphire}$$

An increase in the water of hydrolysis in the sol to 2 moles of water for each mole of ethoxide results in a very different microstructure of  $\text{LiNbO}_3$  film on c-cut sapphire. Figure 11 shows the TEM micrograph of such a film annealed at  $400^\circ\text{C}$  for 1 hour, with the same ramping rate. This film is polycrystalline with a grain size of  $0.5 \mu\text{m}$  and micropores present entrapped within the grains. Similar micropores are also observed at the grain boundaries. X-ray data of the 1:2 film on sapphire showed a strong (0006) reflection of  $\text{LiNbO}_3$  (Fig. 12) indicating that most grains have a preferred growth direction. However, there is no in-plane alignment of the grains and the rotation of the in-plane axes for the  $\text{LiNbO}_3$  grains is evident in the SAD pattern.

#### IV. DISCUSSION

One of the most important results obtained in this study is the fact that water of hydrolysis influences many features including (a) temperature of crystallization, (b) latent heat of crystallization, (c) epitaxy, (d) grain size, and (e) the amount of porosity and pore size in sol-gel derived  $\text{LiNbO}_3$  thin films. In some ways this result may seem surprising because the chemical short range order in the amorphous films derived from the electron diffraction information, was not affected by the amount of water of hydrolysis. Both unhydrolyzed and partially hydrolyzed dried films manifested similar maxima in the short range order. The short range order did not change even after the unhydrolyzed film on glass was treated at  $400^\circ\text{C}$  for 1 hour. However, a similar heat treatment rendered the partially hydrolyzed films on glass and sapphire substrates crystalline.

Short-range order in an amorphous phase is usually very similar to that of the crystal which will grow from the amorphous phase [17]. Prominent atomic pairs in the lithium niobium double ethoxide,  $\text{LiNb}(\text{OC}_2\text{H}_5)_6$ , can be related to the crystal structure of  $\text{LiNbO}_3$ . In this regard it is interesting to consider the results of XRD studies of  $\text{LiNb}(\text{OC}_2\text{H}_5)_6$  and FTIR investigations of amorphous  $\text{LiNbO}_3$  gels by Eichorst and Payne [18]. Their results showed that structure of



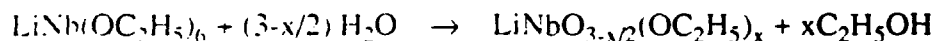
$\text{LiNb}(\text{OC}_2\text{H}_5)_6$  is composed of alternating  $\text{Nb}(\text{OC}_2\text{H}_5)_6$  octahedra linked by severely distorted tetrahedrally coordinated Li atoms. These structural features were maintained during gelation. NMR investigations have shown that it is the Li environment which shows a continuous change with increasing water content until the amount of water reaches the stoichiometric quantity needed for complete hydrolysis (3 moles per mole of ethoxide) [19]. Although NMR results are not reported for the Nb environment with changing amount of water, our results suggest that the Nb octahedra are stable even with changing water concentration in the gel.

The structure of crystalline  $\text{LiNbO}_3$  at temperatures below the ferroelectric Curie temperature (approximately  $1210^\circ\text{C}$ ) consists of planar sheets of oxygen atoms in a distorted hexagonal close-packed configuration. The octahedral interstices formed in this structure are one third filled by lithium atoms, one third filled by niobium atoms, and one third vacant [20]. Since Li atom goes through a change in its coordination state from tetrahedral in the double ethoxide to octahedral in crystalline lithium niobate while Nb remains octahedrally coordinated, it is the Li environment which experiences most of the structural changes during the amorphous to crystalline transformation. If we consider the SAD patterns of amorphous films shown in Figure 2, the interatomic distance  $d_1 \approx 3.7 \text{ \AA}$  corresponds to the theoretical values of the interatomic distances between Nb-Nb and Li-Li pairs in crystalline  $\text{LiNbO}_3$ ,  $3.765 \text{ \AA}$ . The interatomic distance  $d_2 \approx 2.0 \text{ \AA}$  may correspond to the two characteristic Nb-O spacings,  $1.889$  and  $2.212 \text{ \AA}$  [21]. The average Nb-O (bridging) bond length in  $\text{LiNb}(\text{OC}_2\text{H}_5)_6$ , as reported by Eichorst et al using XRD, is  $1.98 \text{ \AA}$  [22]. It is apparent that the distances between these atomic pairs in the amorphous phase change only slightly during crystallization. This indicates that an important criterion for the low temperature crystallization of any phase through sol-gel processing may be the selection of a precursor species which not only has the right stoichiometry but also has a chemical short range order which does not change significantly upon crystallization.

Having described the negligible effect that the water concentration has on the chemical short range order of thin amorphous films of  $\text{LiNbO}_3$  and the similarity in the local atomic arrangement of  $\text{LiNb}(\text{OC}_2\text{H}_5)_6$  to that of crystalline  $\text{LiNbO}_3$ , we are left with the problem of explaining the

dramatic microstructural variations due to changing the amount of water of hydrolysis for crystallized thin  $\text{LiNbO}_3$  films on glass and sapphire. TEM results demonstrate that the amount of water present in the sol markedly influences the grain size and density in crystalline  $\text{LiNbO}_3$  films on glass. The relative rates of hydrolysis and condensation are affected by the amount of water present. These in turn affect the rate of molecular rearrangement that (a) transform the double ethoxide to amorphous lithium niobate and (b) condense the molecules into an interconnected network. These two phenomena, which can be dealt with separately, even though they may occur simultaneously, seem to be responsible for the final differences in grain size and porosity respectively. Three effects of the degree of hydrolysis can be delineated for the purpose of discussion.

(1) The first stage of crystallization is associated with the hydrolysis of the double ethoxide resulting in the formation of amorphous  $\text{LiNbO}_3$  which acts as a building block for crystalline  $\text{LiNbO}_3$ . The concentration of these building blocks in the sol is proportional to the degree of hydrolysis according to the equation,



The possible species produced by this reaction are  $\text{LiNbO}_{1/2}(\text{OC}_2\text{H}_5)_5$ ,  $\text{LiNbO}(\text{OC}_2\text{H}_5)_4$ ,  $\text{LiNbO}_{3/2}(\text{OC}_2\text{H}_5)_3$ ,  $\text{LiNbO}_2(\text{OC}_2\text{H}_5)_2$ ,  $\text{LiNbO}_{5/2}(\text{OC}_2\text{H}_5)$ , and  $\text{LiNbO}_3$ , depending on the amount of water added. In reality, the product of the above reaction is a mixture of these species, though some of them may not exist due to their thermodynamic instability.  $\text{LiNbO}_2(\text{OC}_2\text{H}_5)_2$  and amorphous  $\text{LiNbO}_3$  are known to be stable compounds[18]. Higher water ratios result in a higher concentration of the amorphous  $\text{LiNbO}_3$  species which serve as building blocks for the crystalline phase. Higher water concentrations also result in higher condensation rates as evidenced by the rapid gelation of 1:3 samples. Higher building block concentration and their relatively quick condensation in 1:2 compositions results in large regions having similar structure to crystalline  $\text{LiNbO}_3$ . Since long distance diffusion within the matrix is not required, large scale nucleation

occurs earlier in films with a higher water ratio. Earlier nucleation allows for more time for grain growth in the film synthesized from the higher water concentration sols. Thus, the films with higher water contents have larger grain size due to earlier crystallization.

Additional support for this suggestion is provided by DSC studies where the kinetic parameter  $T_{\text{onset}}$ , characterizing the onset of crystallization of  $\text{LiNbO}_3$ , shows a tendency to decrease as the added water of hydrolysis increased. Also, since the area under the DSC peak is proportional to the heat change involved, the latent heat of crystallization of the 1:2 gel is lower than that of 1:1 gel. Although not conclusive, the accumulated observations indicate that increasing the amount of water of hydrolysis lowers the activation energy for crystallization of  $\text{LiNbO}_3$  which we infer is due to an increased concentration of amorphous  $\text{LiNbO}_3$  building blocks in the sol. This hypothesis could be verified with the help of NMR experiments.

Grain growth to dimensions similar to the 1:2 film occurred in the 1:1 film only at higher temperatures and/or longer soaking times. Unfortunately, this led to interfacial reactions at  $600^\circ\text{C}$ . The presence of a Li deficient phase in 1:1 film on glass is attributed to the elemental diffusion of Li into the substrate interface. Li diffusion is significant at  $600^\circ\text{C}$ , as the activation energy for the diffusion of a small monovalent cation in silicate glasses is generally very low,  $\approx 20 \text{ kJ/g-atom}$  [23]. However, diffusion of Li into the glass substrate does not play a significant role at  $400^\circ\text{C}$  even with long soaking times (4 hours). This is evident from the diffraction pattern of pure  $\text{LiNbO}_3$  in Figure 6b.

(2) The second microstructural difference between the 1:1 and 1:2 amorphous and crystalline films of  $\text{LiNbO}_3$  is the amount of porosity present. Porosity in the film is a function of sol structure [24]. As mentioned earlier, higher water concentrations lead to increased condensation rates. This increases size of precursor species in the sol. The progressive increase in porosity with precursor size is attributed to the rigid gel network which has a tendency to resist compaction during solvent evaporation. Figure 2, which illustrates the amorphous film structure for different water concentration sols, is in agreement with Brinker and coworkers [25]. They hypothesize that weak branching and low condensation rates during film formation allows the

precursor to interpenetrate in response to the decreasing solvent concentration, promoting dense packing and low pore volume.

(3) The third microstructural distinction is associated with epitaxy of  $\text{LiNbO}_3$  on sapphire. Low water concentrations (1:1) yielded epitaxial and single crystalline films whereas higher water concentrations (1:2) yielded polycrystalline films with some preferred orientation. The single crystalline nature of 1:1  $\text{LiNbO}_3$  films but polycrystalline nature of 1:2  $\text{LiNbO}_3$  films on sapphire could be due to the competition between layer-by-layer solid phase epitaxy and random crystallization. The former phenomenon involves not only heteroepitaxial nucleation at film-substrate interface but also subsequent homoepitaxial film growth on this initially nucleated layer. To ensure that the film retains its single crystal character, no two dimensional nucleation of misoriented crystallites should occur [26]. This requires slow nucleation but a rapid lateral spreading rate. Braunstein et al [27] were able to promote layer-by-layer solid phase epitaxy over random crystallization of sol-gel derived  $\text{SrTiO}_3$  on (100)  $\text{SrTiO}_3$  substrate by using high annealing temperatures, where surface diffusion was rapid. In our films, the lateral spreading rate is kinetically limited due to the low temperature of crystallization. The activation energy for heteroepitaxial nucleation on (0001) sapphire is slightly lower than that for random nucleation of  $\text{LiNbO}_3$  for 1:1  $\text{LiNbO}_3$  films, validated by the observation of single crystal epitaxy on (0001) sapphire instead of polycrystalline films as was the case for glass substrates under the same annealing conditions. This difference in activation energy is narrowed for 1:2  $\text{LiNbO}_3$  films, where we postulate that higher concentration and aggregation of amorphous  $\text{LiNbO}_3$  building blocks lowers the temperature for random nucleation. Heteroepitaxial nucleation should also occur concurrently with enhanced nucleation of random nuclei on the substrate surface in 1:2 films. Activation energy for crystallization is higher in 1:1 than 1:2 so the nucleation rate would be lower in 1:1 than 1:2. Therefore, we expect that epitaxy is easier for 1:1 films due to the lower random nucleation rate and the similar lateral spreading rate for 1:1 and 1:2 films.

The lateral growth of heteroepitaxial nuclei in 1:1 films followed by homoepitaxial growth in subsequent layers results in dense single crystalline  $\text{LiNbO}_3$  films. However, since multiple

heteroepitaxial nuclei are involved, they grow independently as islands. When they impinge, any mismatch is accommodated by the generation of defects such as stacking faults, twins, and dislocations as can be seen in Figure 8 and 9. In Figure 10, Moiré fringes revealed the periodicity of misfit between the  $\text{LiNbO}_3$  and sapphire. The spacing of the Moiré fringes corresponds to the predicted value for  $(11\bar{2}0)$   $\text{LiNbO}_3$  on  $(11\bar{2}0)$  sapphire. The presence of dislocations at the interface generated during film growth are also revealed in the Moiré fringe pattern, visible as terminating fringes. An example of such a fringe is identified by the arrow in figure 10a. These results also substantiate the interface nucleation for 1:1 films.

One final point that we wish to consider is the texturing of  $\text{LiNbO}_3$  due to anisotropic surface energies. In our TEM studies on  $\text{LiNbO}_3$  powders, we noted that at higher temperatures ( $600^\circ\text{C}$ ) the growing particles further minimize their surface energy by acquiring faceted shapes. The face plane, plane of lowest surface energy, is the close packed  $(0001)$  plane for  $\text{LiNbO}_3$ . In order to increase the surface area of  $(0001)$  plane, the growth of  $\text{LiNbO}_3$  crystal in  $[0001]$  direction is very slow and it grows rapidly in the directions which are parallel to  $(0001)$  plane. This is evident from the presence of hexagonal particles at  $600^\circ\text{C}$ . Matsunaga et al [29] have also reported the tendency of  $\text{LiNbO}_3$  films (deposited by ion plating) on glass substrates to orientate with the c-axis normal to the surface at  $500^\circ\text{C}$ . As mentioned earlier, for the growth of epitaxial films rapid lateral spreading rate is desired vs a high nucleation rate. It is possible that low temperature heteroepitaxial growth of  $\text{LiNbO}_3$  is facilitated when its  $[0001]$  direction is perpendicular to the substrate. It is interesting to mention here that Nashimoto and Cima [9] only had success in growing heteroepitaxial films on  $(11\bar{2}0)$  sapphire at  $400^\circ\text{C}$  when they used unhydrolyzed sols. They reported  $(11\bar{2}0)$  oriented but polycrystalline growth of 1:1  $\text{LiNbO}_3$  films.

## V. CONCLUSIONS

(1) Crystallization in double ethoxide derived  $\text{LiNbO}_3$  was observed to begin in bulk gels at temperatures as low as  $200^\circ\text{C}$ . At higher temperatures ( $600^\circ\text{C}$ ), hexagonal faceting of crystalline particles occurred with side facets being the first order prism planes and the large area faces the basal plane.

(2) Water of hydrolysis appeared to negligibly affect the chemical short range order of the amorphous  $\text{LiNbO}_3$  films but DSC results showed a lower temperature of crystallization for higher water content sols. It is postulated that higher amounts of water lead to larger regions of  $\text{LiNbO}_3$  building blocks in the sol which lower the temperature and activation energy of crystallization.

(3) Sols deposited on glass substrates having low ethoxide to water ratio yielded dense and smooth polycrystalline films, whereas, rough, porous films with a large grain size resulted from the use of sols with increased water of hydrolysis. Earlier crystallization allowed for more grain growth.

(4) Low water content sols promoted epitaxial growth of dense  $\text{LiNbO}_3$  on sapphire with nucleation at the substrate interface. The ease of random nucleation in high water content sols produced polycrystalline films with some oriented growth.

## VI. ACKNOWLEDGMENTS

This work has been supported through a grant from the Air Force Office of Scientific Research under contract number 49620-89-C-0050. Center for Interfacial Engineering is acknowledged for the use of CM30 TEM and Nanoscope II AFM.

## LIST OF FIGURES

**Figure 1:** Cryogenic transmission electron micrograph illustrating the microstructure of a 1:2  $\text{LiNb}(\text{OC}_2\text{H}_5)_4/\text{H}_2\text{O}$  sol at 75% of gelation time. SAD pattern represents the amorphous nature of the sol.

**Figure 2:** Amorphous  $\text{LiNbO}_3$  films with ethoxide/water ratios of (a) 1:0, (b) 1:1, and (c) 1:2. These images show nanometer scale porosity, which increases with increasing amount of water in the sol.

**Figure 3:** Water of hydrolysis dependence of DSC curves for various  $\text{LiNbO}_3$  gels.

**Figure 4:** Transmission electron micrographs and corresponding SAD patterns of  $\text{LiNbO}_3$  gels (a)  $200^\circ\text{C}$ , (b)  $450^\circ\text{C}$ , and (c)  $600^\circ\text{C}$ .

**Figure 5:** Atomic force micrographs of  $\text{LiNbO}_3$  films on glass substrates with ethoxide/water ratios of (a) 1:0, (b) 1:1, and (c) 1:2. All the films were annealed at  $400^\circ\text{C}$  for 1 hour.

**Figure 6:** Variation in microstructure with ethoxide to water ratio for  $\text{LiNbO}_3$  films on glass substrates (a) 1:0, (b) 1:1, and (c) 1:2. All the films were annealed at  $400^\circ\text{C}$  for 1 hour.

**Figure 7:** Crystallized  $\text{LiNbO}_3$  thin films on glass: (a) effect of higher temperature,  $600^\circ\text{C}$  for 1 hour and (b) effect of longer soaking time,  $400^\circ\text{C}$  for 4 hour.

**Figure 8:** (a) Bright field and (b) dark field images of single crystal 1:1  $\text{LiNbO}_3$  thin film on (0001) sapphire substrate, annealed at  $400^\circ\text{C}$  for 1 hour.

Figure 9: Twinning in  $[1\bar{1}00]$  direction as evidenced in the SAD pattern of 1:1  $\text{LiNbO}_3$  thin film on sapphire. Zone axis =  $[0001]$ .

Figure 10: (a) Moiré fringes revealing the misfit between (0001) oriented 1:1  $\text{LiNbO}_3$  film on (0001) sapphire. The arrow indicates a terminating fringe. (b) SAD pattern with electron beam parallel to sapphire  $[0001]$  zone axis confirming epitaxial nature of the 1:1  $\text{LiNbO}_3$  film.

Figure 11: TEM image of a 1:2  $\text{LiNbO}_3$  thin film on (0001) sapphire. Intergranular and intragranular porosity can be seen in the micrograph. Note the polycrystalline nature of this film in contrast to the film in Figure 7.

Figure 12: XRD patterns of  $\text{LiNbO}_3$  films on (0001) sapphire showing effect of water of hydrolysis.



## REFERENCES

1. R.S. Weis and T.K. Gaylord, Appl. Phys. A **37**, 191 (1985).
2. K. Nassau, H. Levinstein, and G. Loiacono, J. Phys. Chem. Solids **27** 989 (1966).
3. K. Nassau and H. Levinstein, Appl. Phys. Lett. **7** 69 (1965).
4. M.M. Abouelleil and F.J. Leonberger, J. Am. Ceram. Soc. **72** 311 (1989).
5. G. Griffel, S. Ruschin, A. Hardy, M. Itzkovitz and N. Croitoru, Thin Solid Films **126** 185 (1985).
6. A. Okada, Ferroelectrics **14** 739 (1976).
7. S. Hirano and K. Kato, J. Non-Cryst. Solids **100** 538 (1988).
8. D.P. Partlow and J. Gregg, J. Mater. Res. **2** 595 (1987).
9. K. Nashimoto and M.J. Cima, Materials Letters **10** 348 (1991).
10. C.C. Hseuh and M.L. Mecartney, J. Mater. Res. **6** 2208 (1991).
11. J.L. Keddie and E.P. Giannelis, J. Am. Ceram. Soc. **74** 2669 (1991).
12. C.D.E. Lakeman and D.A. Payne, J. Am. Ceram. Soc. **75** 3091 (1992).
13. V. Joshi, G.K. Goo, and M.L. Mecartney in *Better Ceramics through Chemistry V*, edited by M.J. Hampden-Smith, W.G. Klemperer, and C.J. Brinker (Mater. Res. Soc. Symp. Proc. **271**, Pittsburgh, PA, 1992), p. 377.
14. S. Hirano and K. Kato, Advanced Ceramic Materials **3** 503 (1988).
15. J.K. Bailey, J.R. Bellare, and M.L. Mecartney in *Specimen preparation for transmission electron microscopy of materials*, edited by J.C. Bravman, R.M. Anderson, and M.L. McDonald (Mater. Res. Soc. Symp. Proc. **115**, Pittsburgh, PA, 1988), p. 69.
16. S.M. Hues, R.J. Colton, E. Meyer, and H.J. Güntherodt, MRS Bulletin **XVIII** (1) 41 (1993).
17. B.E. Warren, J. Am. Ceram. Soc. **17** 249 (1934).
18. D.J. Eichorst and D.A. Payne in *Better Ceramics through Chemistry IV*, edited by B.J.J. Zelinski, C.J. Brinker, D.E. Clark, and D.R. Ulrich (Mater. Res. Soc. Symp. Proc. **180**, Pittsburgh, PA, 1990), p. 669.

19. D.J. Eichorst, K.E. Howard, and D.A. Payne, unpublished results.
20. A. Rauber in *Current Topics In Materials Science*, edited by E. Kaldis (North-Holland, Amsterdam 1978) p. 481.
21. A.M. Prokhorov and Y. S. Kuzminov, *Physics and Chemistry of Crystalline Lithium Niobate* (Adam Hilger, Bristol and New York, 1990) p. 18.
22. D.J. Eichorst, D.A. Payne, S.R. Wilson, and K.E. Howard, *Inorg. Chem.* **29** 1459 (1990).
23. W.D. Kingery, H.K. Bowen, and D.R. Uhlmann, *Introduction to Ceramics* (John Wiley & Sons, New York, 1976) 2nd ed., pp. 257, 263.
24. C.J. Brinker and G.W. Scherer, *Sol-Gel Science* (Academic Press, New York, 1990) pp. 799, 814.
25. C.J. Brinker, A.J. Hurd, and K.J. Ward in *Ultrastructure Processing of Advanced Ceramics*, eds. J.D. Mackenzie and D.R. Ulrich (Wiley, New York, 1988) p. 223.
26. W.A. Tiller, *The Science of Crystallization - Microscopic Interfacial Phenomena* (Cambridge University Press, New York, 1991) pp. 171, 175.
27. G. Braunstein, G.R. Raz-Pujalt, M.G. Mason, T. Blanton, C.L. Barnes, and D. Margevich, *J. Appl. Phys.* **73** 961 (1993)
28. H. Matsunaga, H. Ohno, Y. Okamoto, and Y. Nakajima, *J. Cryst. Gro.* **99** 630 (1990).

Figure 1

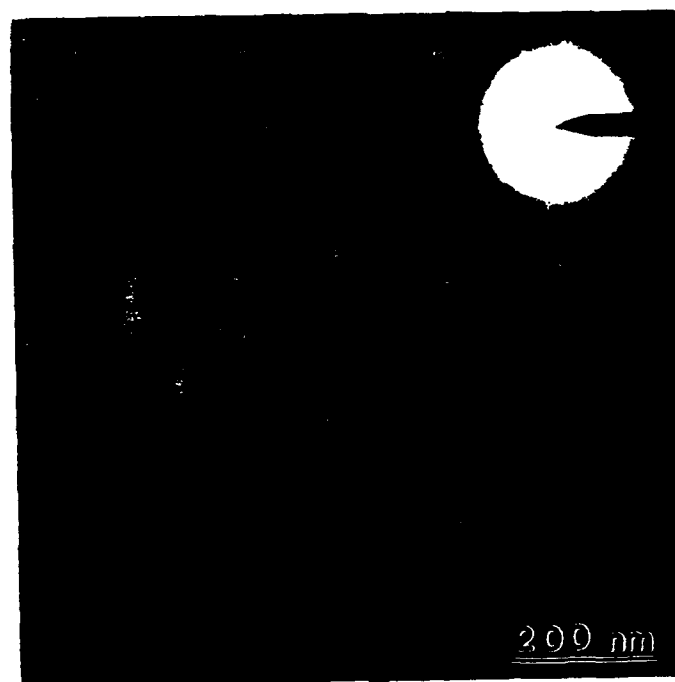


Figure 2

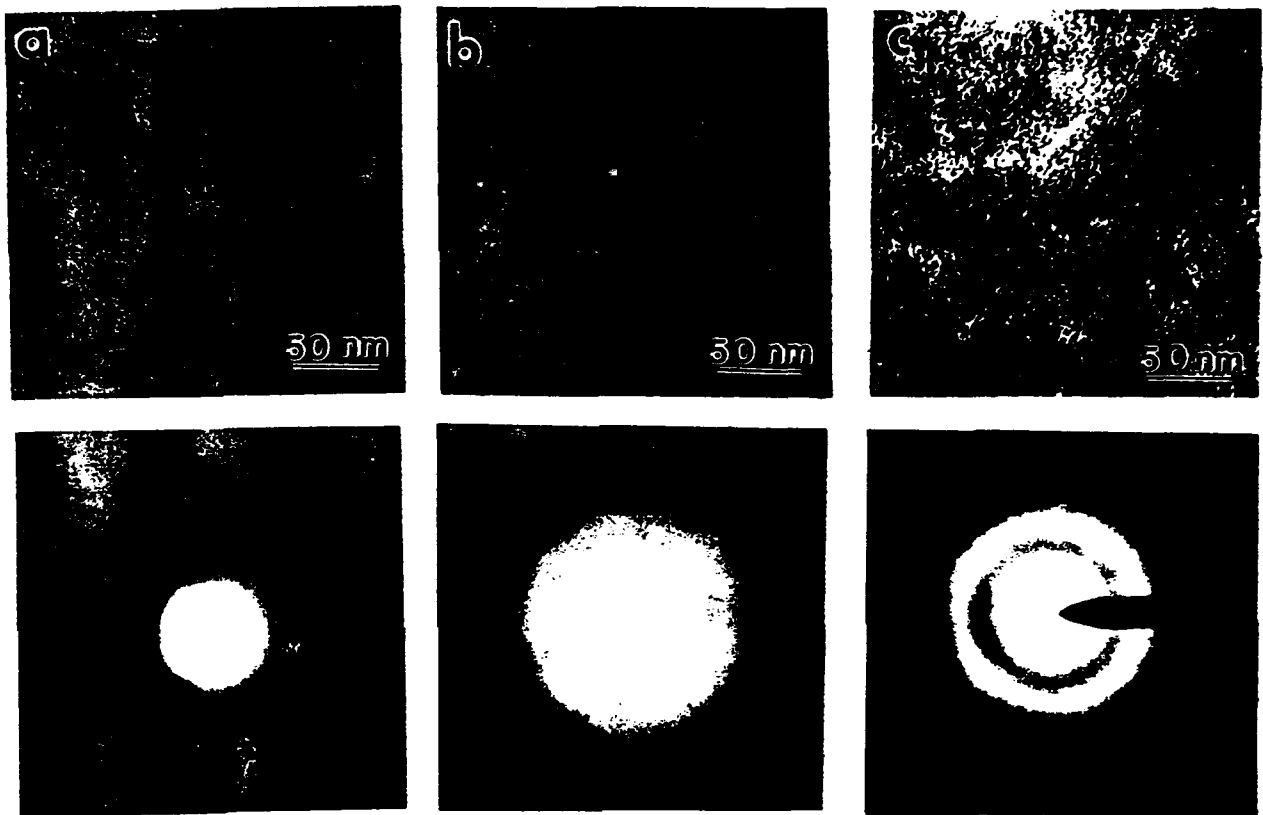
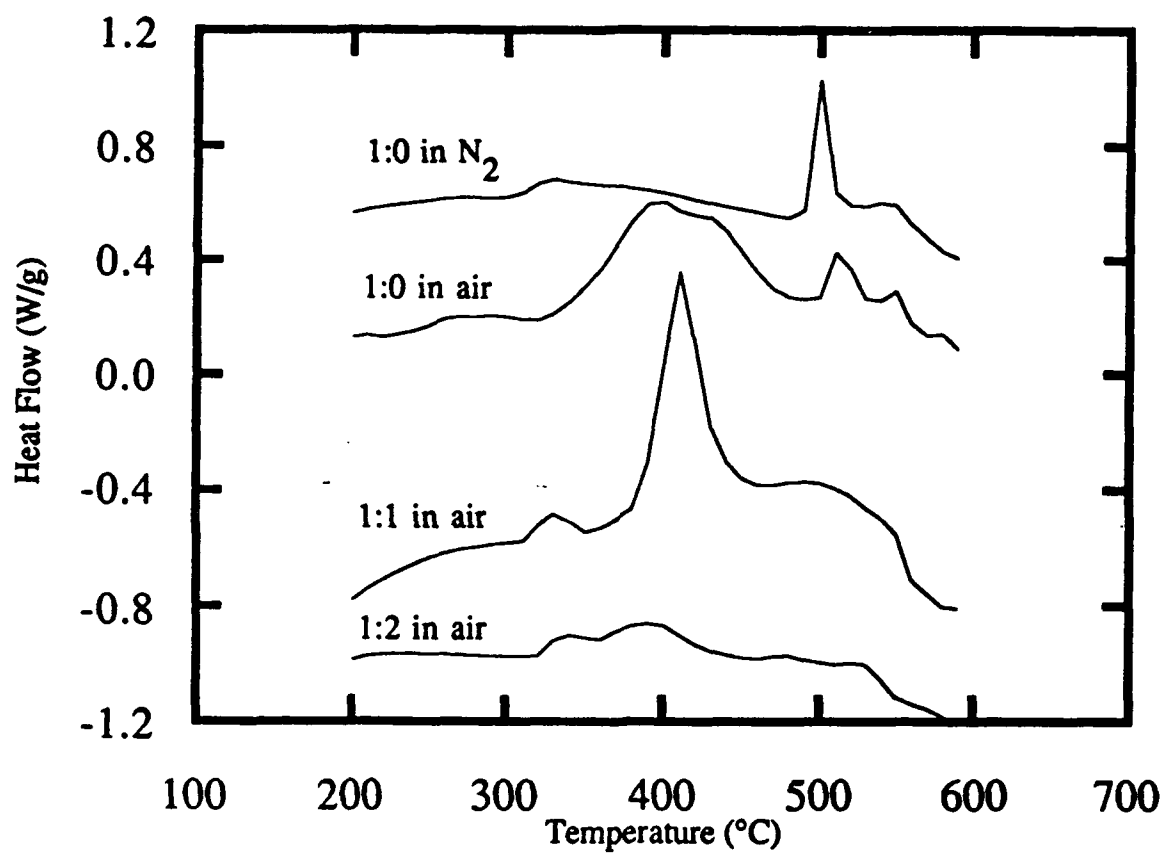


Figure 3



**Figure 4**

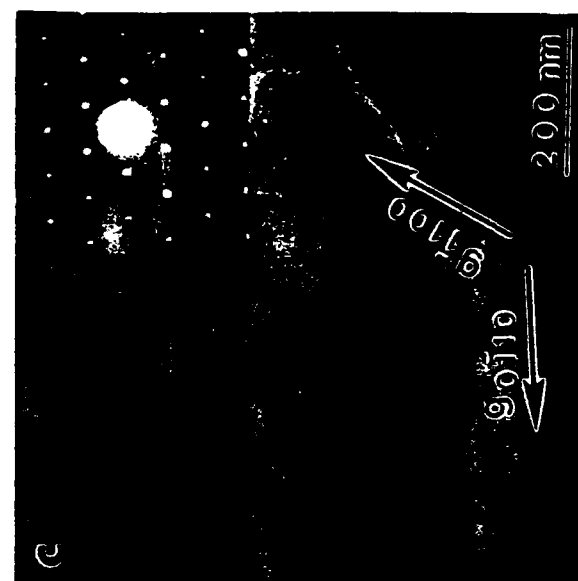


Figure 5

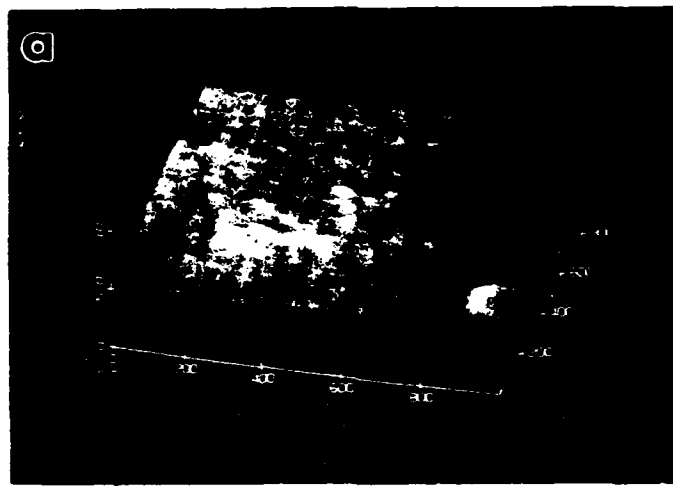


Figure 6

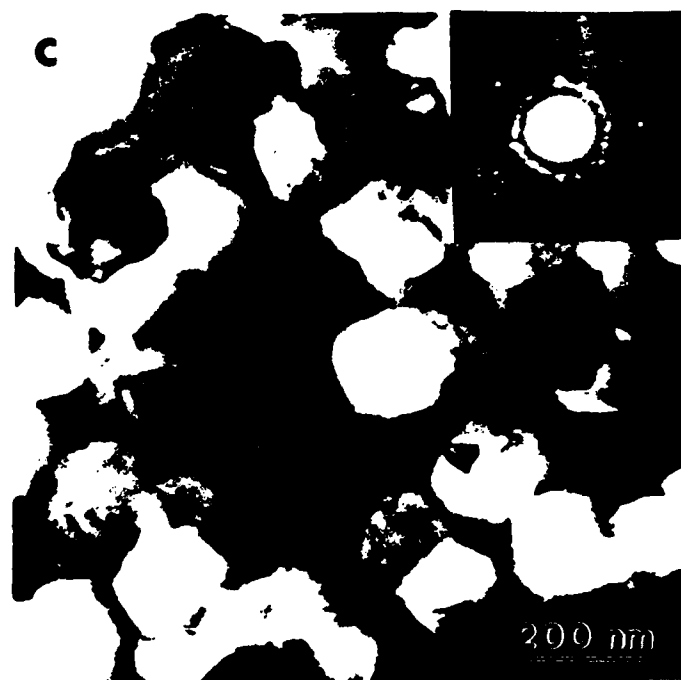
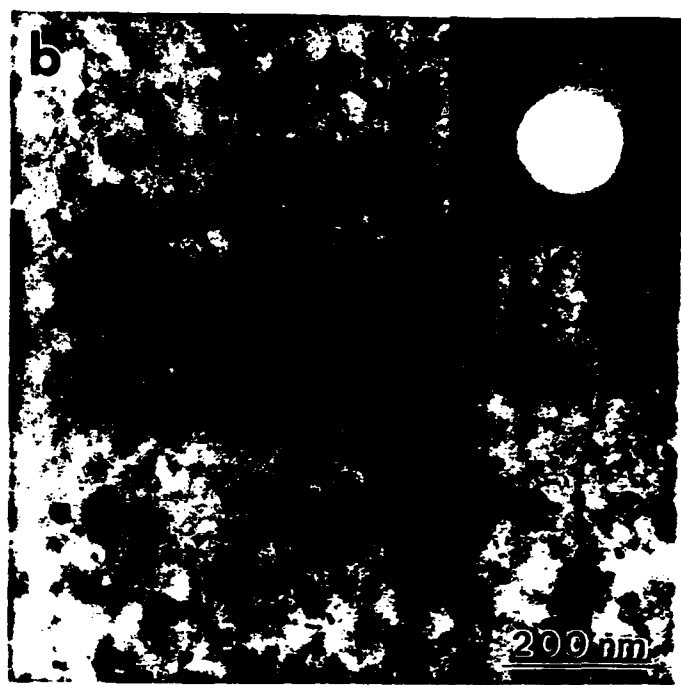
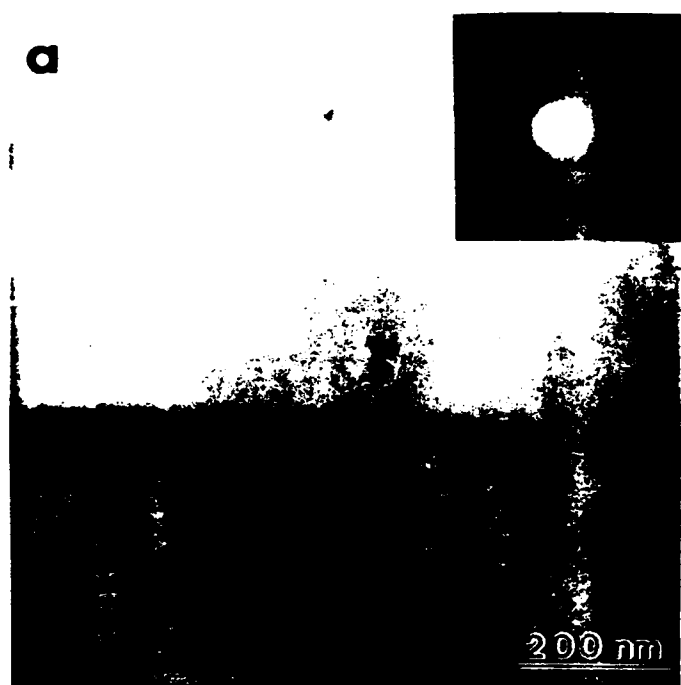




Figure 7

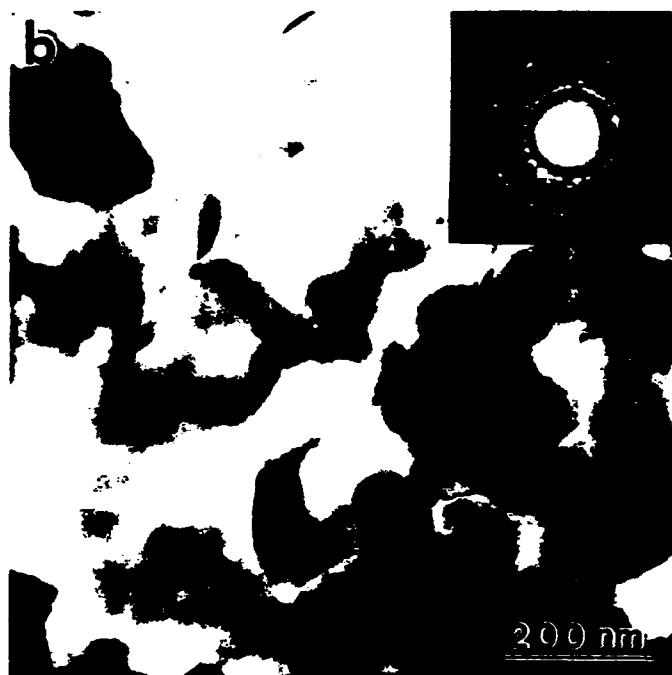
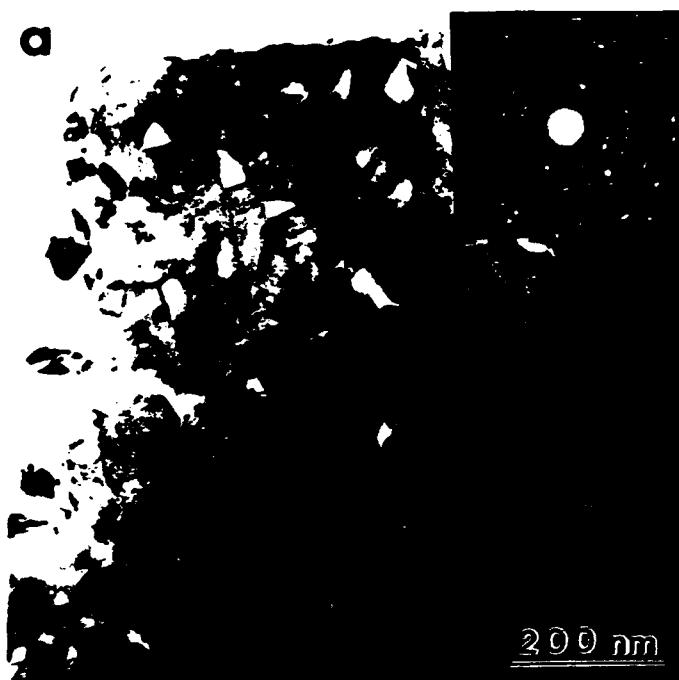


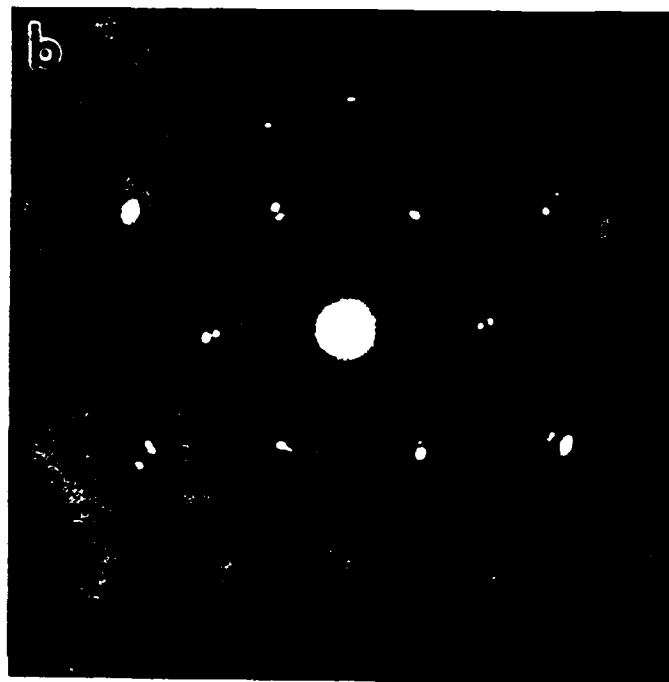
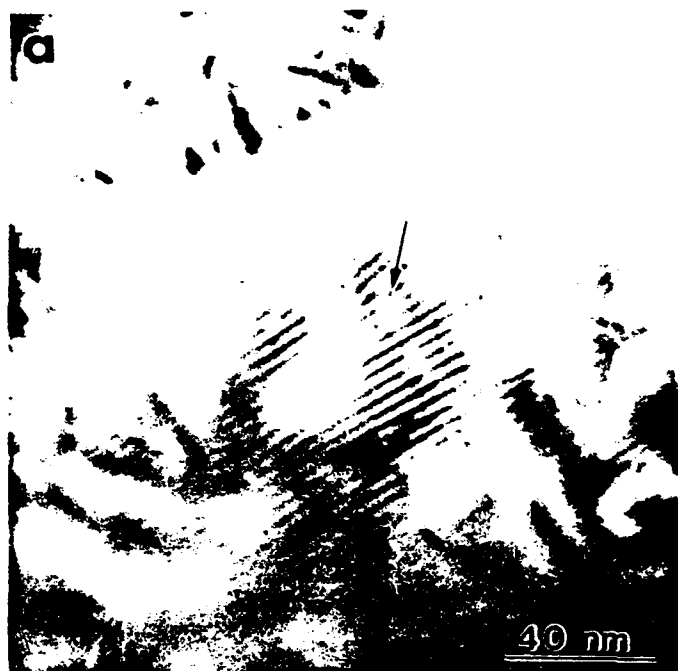
Figure 8



Figure 9



Figure 10



**Figure 11**

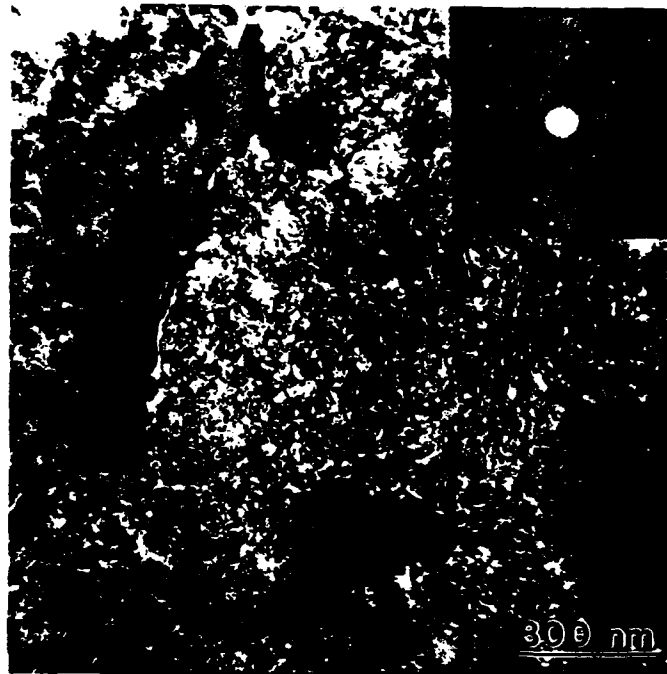
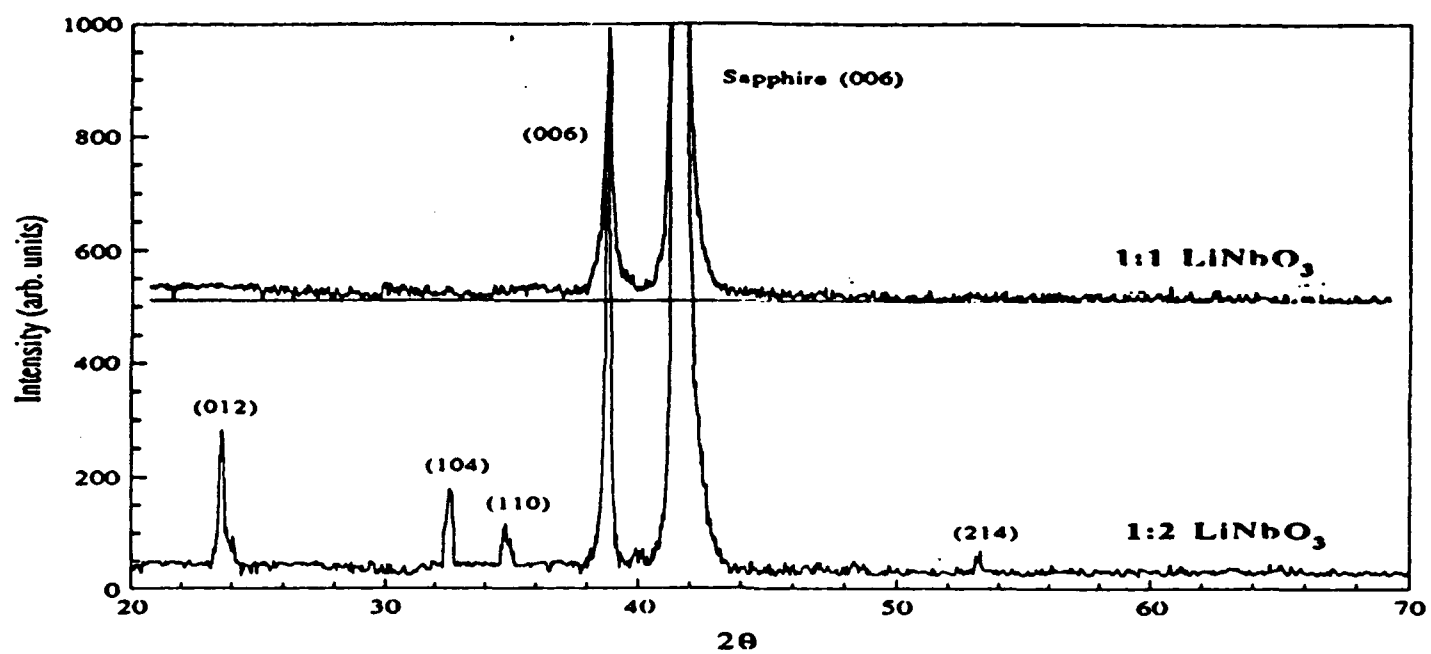


Figure 12



# LITHIUM NIOBATE THIN FILMS ON AMORPHOUS CARBON SUBSTRATES

Martha L. McCartney (prof.) and Vikram Joshi (grad. student)

Department of Mechanical Engineering & Materials Science

University of California, Irvine

## *Abstract*

Lithium niobium ethoxide sols were deposited onto carbon support films. Increased water of hydrolysis enhanced crystallization. Transmission electron microscopy studies of ultrathin layers of hydrolyzed sols on carbon substrates produced preliminary evidence of room temperature crystallization.

## *Experimental*

In addition to glass and sapphire substrates, carbon support films were also used for the deposition of  $\text{LiNbO}_3$  films. The substrates (Ted Pella, Inc. Redding CA) were in the form of thin formvar films covered with a light layer of evaporated carbon and supported on TEM copper grids (200 mesh). Thickness of the formvar layer was 50 nm and that of amorphous carbon layer was 10 nm. Lithium niobium ethoxide ( $\text{LiNb}(\text{OC}_2\text{H}_5)_6$ ) was prepared according to the method described in the accompanying paper. Sols were hydrolyzed with different amounts of water. Four different ethoxide to water ratios were used: 1:0 (unhydrolyzed sol), 1:1, 1:2, and 1:3. Extremely small amount of sols (5  $\mu\text{l}$ ) were deposited on the substrates using a micropipette in a controlled environmental chamber. The chamber was completely saturated with ethanol vapor in order to avoid rapid evaporation of the solvent. After deposition, the excess sol was removed by using a blotting paper. This left an electron transparent thin layer of sol on the carbon surface. During condensation and evaporation, the gel further shrank, leaving behind extremely thin sections of the film. These thin regions were studied using a 200keV TEM (Philips CM20). A double tilt stage cooled with  $\text{LN}_2$  was used to minimize beam heating effects. The results of these experiments are described below.

## *Results*

Figure 1 shows the microstructure of unhydrolyzed (1:0) film on amorphous carbon substrate. The selected area diffraction (SAD) pattern indicates amorphous nature of this film and the image shows extremely fine porosity on the order of 1 nm. The uniform contrast in the micrograph suggests that the film is very uniform in thickness. Shrinkage due to a uniform rate of evaporation of solvent through out the thin film resulted in a uniform thickness.

When the sols were partially hydrolyzed, gelation followed by evaporation led to cracking and shrinkage of the gel. This left a thin (several hundred angstrom) gel residue on the carbon support film between regions of thick dense gel. These thin film regions on amorphous carbon produced partially crystallized films of  $\text{LiNbO}_3$  at room temperature. Since the films were examined at liquid nitrogen temperature, and crystallized regions were apparent at the onset of the TEM examinations and did not change during examination by TEM, we have inferred that beam heating was not responsible for the crystallization.

The crystalline nature of the film varied depending upon the amount of water used for hydrolyzing the sols. Figure 2 shows bright and dark field images of a 1:1 film. The electron diffraction pattern shows the polycrystalline nature of the film. All the rings indexed to  $\text{LiNbO}_3$   $d$  spacings. There are few missing rings in the diffraction pattern indicating some degree of orientation of the tiny crystallites in the 1:1 film. The size of these crystallites ranges between 30 - 60 nm. Figure 3 shows the microstructure of 1:2 film. Two different morphology of crystallites can be seen: tiny round crystallites less than 20 nm in size and rod shaped crystallites which are about 20 nm wide and 100 to 200 nm long. Figure 2b and 2d show dark field images of Figure 2a and 2c respectively. The circles in the corresponding SAD patterns indicate the portion of the electron diffraction pattern used to obtain the dark field image. It is evident that the two different crystallites have nucleated with different orientation. The diffraction ring with largest  $d$  spacing (3.76 Å) is responsible for the roundish crystallites. This is close to  $\text{LiNbO}_3$   $d_{012}$  spacing of 3.754 Å. The rod shaped crystallites exhibit orientation corresponding to 2nd and 3rd diffraction rings (inset Fig. 3c). The calculated  $d$  spacing of these rings are 2.32 and 2.20 Å respectively. The first corresponds to  $\text{LiNbO}_3$   $d_{006}$  spacing of 2.311 Å but the second  $d$  spacing of 2.20 Å does not match closely with any theoretical  $d$  spacings of  $\text{LiNbO}_3$ . It lies between  $d_{113}$  (2.249) and  $d_{202}$  (2.122). It is difficult to say at this point, whether the presence of this ring is due to a distorted  $\text{LiNbO}_3$  lattice or it indicates the presence of a second phase. Note that this ring is absent in SAD pattern of 1:1 films (Fig. 2a). The second and third rings are so close that it was not possible to separate them even with the smallest objective aperture.

A 1:3 deposited film had no round or rod shaped particles but selected regions were single crystalline in nature. One such region is shown in Figure 4. The region is single crystalline and the zone axis is [0001]. Moiré fringes can also be seen due to rotation of two overlying  $\text{LiNbO}_3$  grains.

### Conclusions

The results indicating enhanced crystallization with increasing water of hydrolysis are consistent with our prior results on glass and sapphire. However, these observations are extremely fascinating as they imply room temperature crystallization of  $\text{LiNbO}_3$  from liquid



precursors. We are beginning the patent application process while we are continuing experiments to focus on the role of carbon in the crystallization of ultrathin films of lithium niobate gels.

### List of Figure

1.  $\text{LiNbO}_3$  thin film on amorphous carbon substrate from unhydrolyzed sol.
2.  $\text{LiNbO}_3$  thin film on amorphous carbon substrate from partially hydrolyzed sol (ethoxide to water ratio of 1:1); (a) bright field and (b) dark field.
3.  $\text{LiNbO}_3$  thin film on amorphous carbon substrate from 1:2 sol; (a) bright field, (b) dark field of 3a, (c) magnified bright field image of the film, and (d) dark field of 3c. The circles in the SAD patterns identify the region of the diffraction pattern responsible for the dark field images.
4. A section of a 1:3  $\text{LiNbO}_3$  thin film on amorphous carbon substrate showing a single crystalline region. Such grains were scattered through out the ultrathin regions of the film.

Figure 1

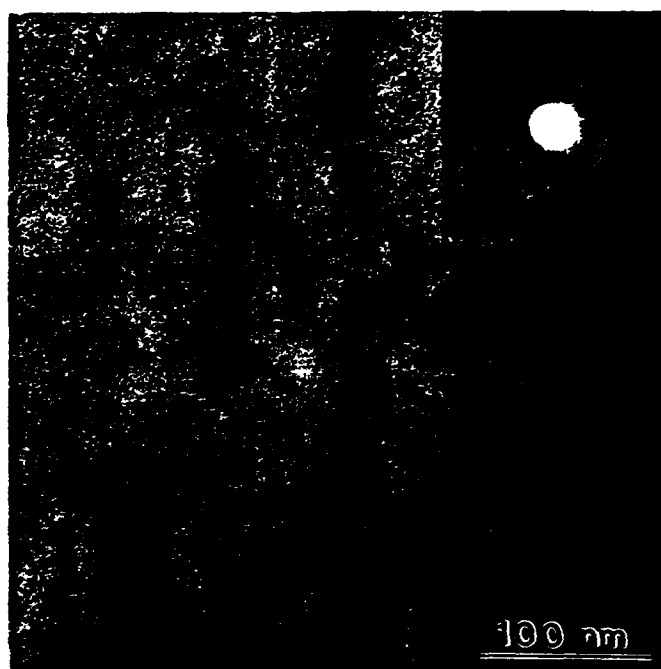


Figure 2

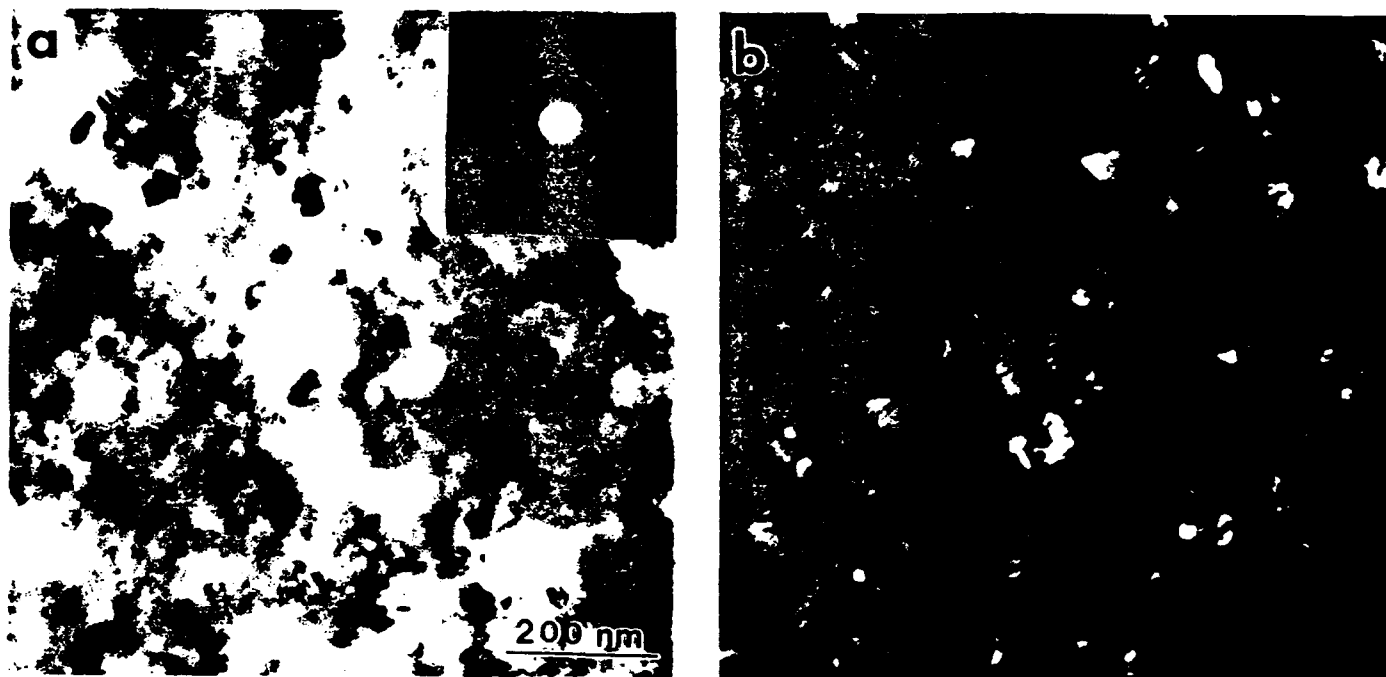


Figure 3

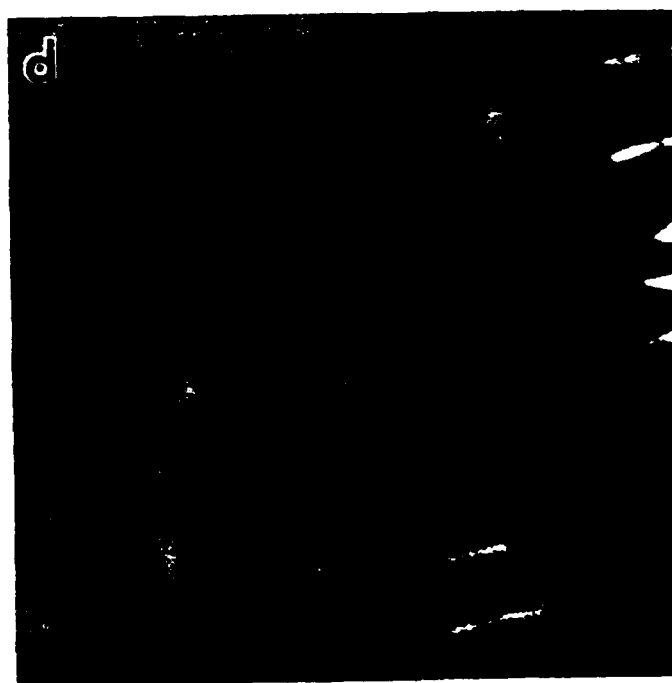
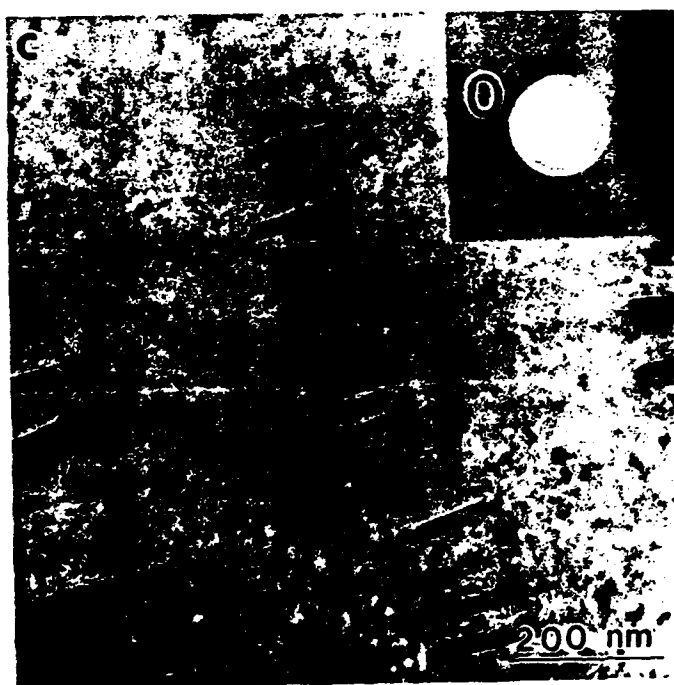
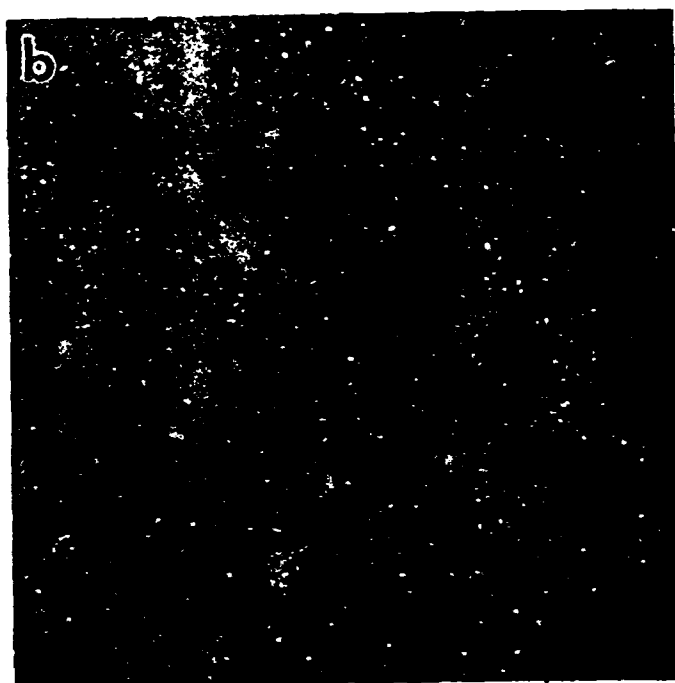
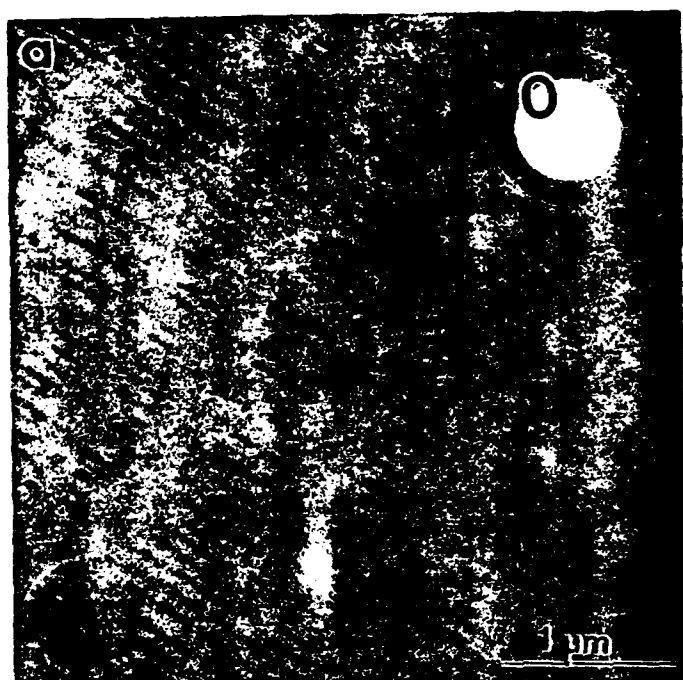
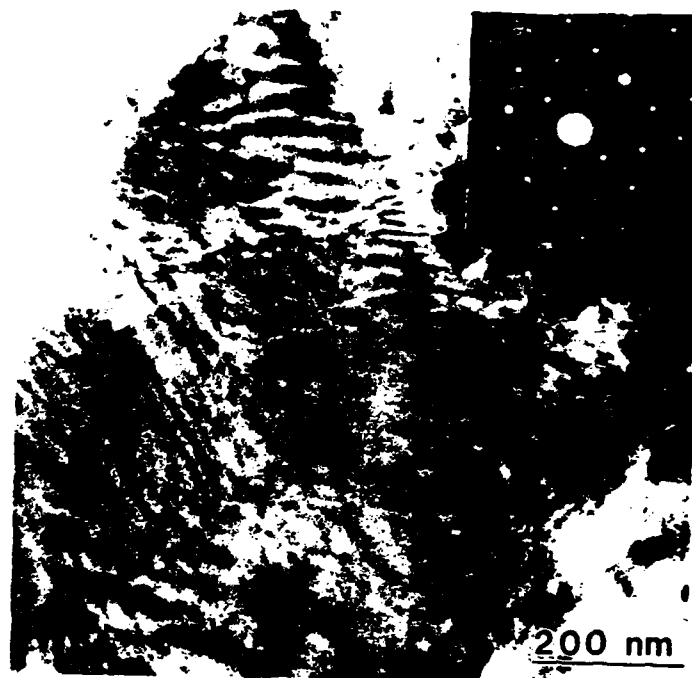


Figure 4



## MICROSTRUCTURAL VARIATIONS IN SOL-GEL PROCESSED LITHIUM NIOBATE THIN FILMS

VIKRAM JOSHI\*, GRACE K. GOO\*\*, AND MARTHA L. MCCARTNEY\*\*

\*University of Minnesota, Dept. of Chemical Engineering and Materials Science, Minneapolis, MN 55455

\*\*University of California at Irvine, Materials Science and Engineering Program, Irvine, CA 92717

### ABSTRACT

LiNbO<sub>3</sub> thin films were deposited by dip coating Li-Nb alkoxide solutions onto silicate glass substrates and single crystal sapphire substrates. Microstructural characterization using transmission electron microscopy (TEM) showed significant differences in film microstructures dependent on the initial solution chemistry. Fully crystalline films could be obtained after heat treatments at 400°C in air. The grain size and porosity were dependent on the amount of water of hydrolysis in the alkoxide sol. The higher the water content, the larger the grain size and porosity. Crystallization studies of nucleation and growth of LiNbO<sub>3</sub> for films heat treated from 300-600°C indicated that higher temperatures or long soak times generated large faceted grain structures. Single crystalline films were obtained on (0001) sapphire substrates.

### INTRODUCTION

Lithium niobate is a promising material for integrated optic devices due to its fast response time and low absorption. Applications include usage in dielectric waveguides, Q-switches, integrated optics and many others. The interest in preparing the lithium niobate by sol-gel routes is due to the homogeneity and high purity that can be achieved in the final product. Thin films can be easily prepared by sol-gel processing, at relatively low temperatures as compared to traditional film preparations [1-6]. Work performed by Nashimoto and Cima [6] on the development of LiNbO<sub>3</sub> thin films using X-ray techniques has shown that the amount of water of hydrolysis plays an important role in the resulting film structure. Other studies have shown that crystallization of the amorphous lithium niobate gel initiated at temperatures as low as 200°C [7]. Changes in particle morphology were observed at higher processing temperatures. The goal of this study is to observe, via TEM, the effects of varying processing temperature, soak time, amount of water of hydrolysis, and substrate with respect to the microstructural development of lithium niobate thin films.

### EXPERIMENTAL PROCEDURE

The procedure for obtaining the lithium niobate complex alkoxides are given in reference [3]. Thin films were dip coated onto substrates and heating was performed at 10°C/min. in air. To study the effect of water of hydrolysis, three different alkoxide to water ratios were used; namely, 1:0, 1:1, and 1:2. To study the effect of temperature, samples with a 1:1 alkoxide to water ratio were used with soak temperatures of 300, 400, 500, and 600°C for 60 minutes. To study the effect of soak time, samples with a 1:1 alkoxide to water ratio were used and held at 400°C for 10, 30, 60, 120, and 240 minutes. All these samples were prepared using glass substrates and were quenched in air following the heat treatment. To study the effect of different substrates on thin film growth, single crystal sapphire (0001 orientation) substrates were used.

A modified TEM specimen preparation technique was developed in order to eliminate any damage or artifacts caused by ion milling. To study films in plan view, conventional TEM specimen preparation involves the deposition of the film followed by mechanical thinning and ion milling from one side. The ion milling process may result in introducing artifacts or film damage. Peel off of the film from the substrate was a significant problem. For the technique used in this study, the substrates were initially thinned to perforation before film deposition. A similar technique has been employed previously for studying nucleation and growth of thin films grown by vapor phase deposition [8]. Figure 1 shows schematics for the two different

techniques for TEM sample preparation of thin films. It can be seen that the specimen prepared by using the modified technique produces a thicker film in the electron transparent region. Figure 2 shows TEM micrographs comparing the microstructure of the films synthesized with similar processing conditions (1:1 alkoxide to water ratio, 400°C, 60 min.) but with the two different TEM specimen preparation techniques described above. The grain size for both films is similar; however, the film deposited on the pre-thinned substrate shows cracking. The perforation in the pre-thinned substrate acts as an edge, and dip coated films in general are not uniform or continuous at the edge of a substrate.

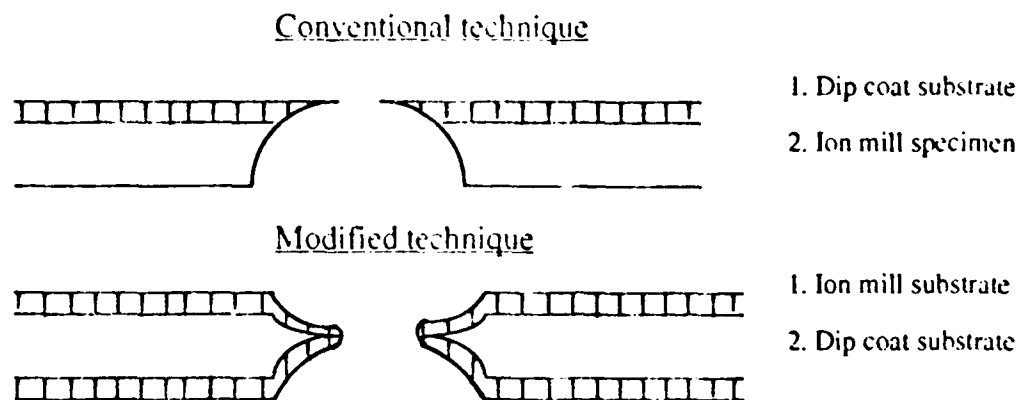


Figure 1: Schematic illustration of the two different techniques for TEM sample preparation of thin films.

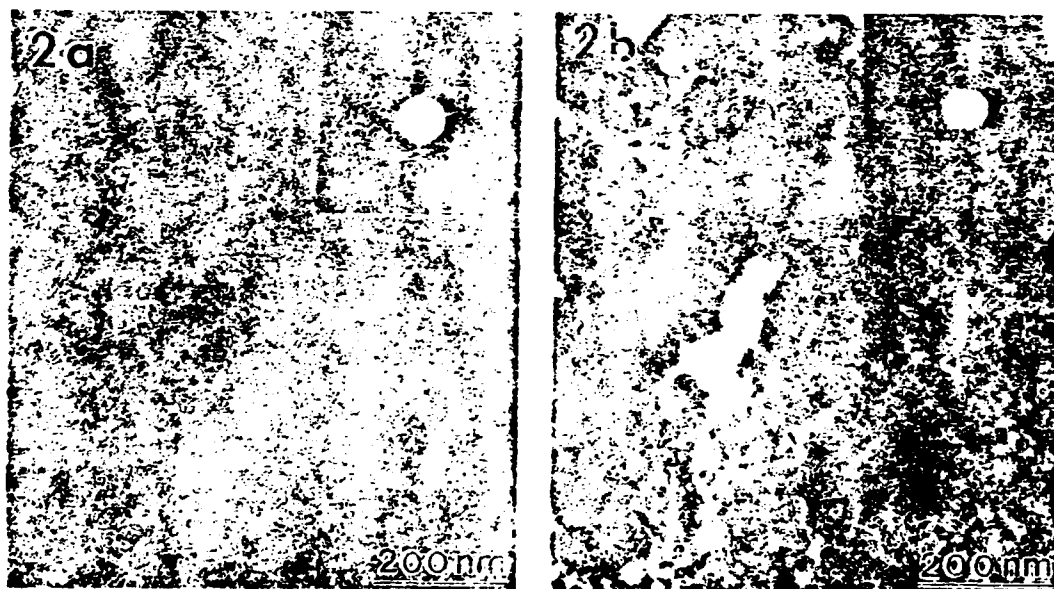


Figure 2: Microstructural comparison of  $\text{LiNbO}_3$  thin films synthesized with similar processing conditions (1:1 alkoxide to water ratio, 400°C, 60 min.) but with the two different TEM specimen preparation techniques; (a) conventional, (b) modified.



## RESULTS AND DISCUSSION

### Effect of alkoxide to water ratio

Figure 3 shows the TEM results with corresponding SAD patterns for varying the alkoxide to water ratio for samples treated at 400°C for 60 minutes on glass substrates. TEM specimens for these films were prepared by conventional technique. The sample with 1:0 alkoxide to water ratio is amorphous with no pores visible. The sample with 1:1 alkoxide to water ratio gives extremely refined crystallites on the order of 30 nm, and the film is very dense. As the alkoxide to water ratio increases (1:2), the size of the crystallites increases (150 nm) as well as the formation of porous network in the thin film. The results indicate that not only is hydrolysis critical for crystallization but the amount of water also plays an important role in determining the grain size and porosity of the film.

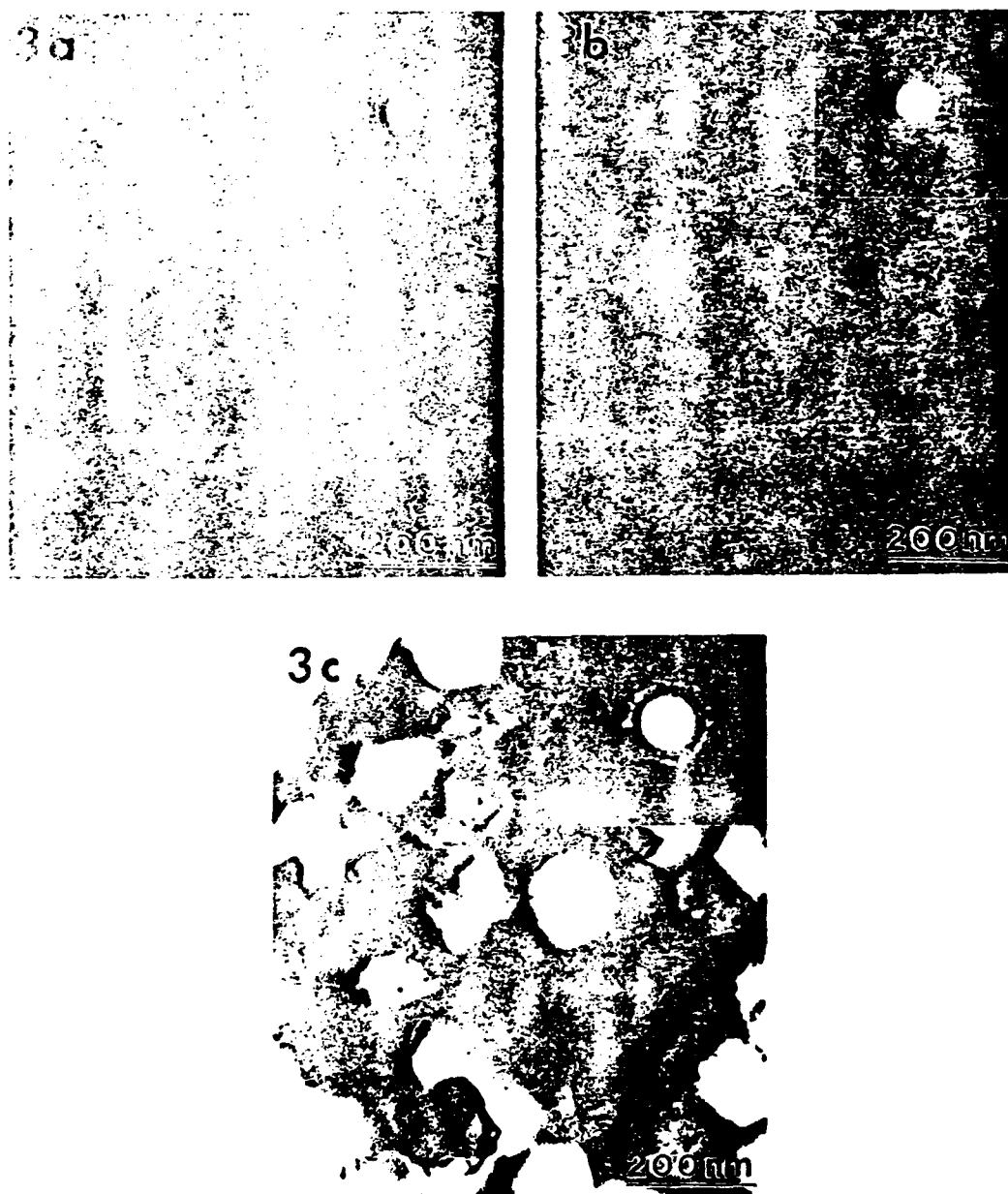


Figure 3: Film heated at 400°C for 60 min; (a) 1:0, (b) 1:1, and (c) 1:2 alkoxide/water ratio.

### Effect of soak temperature

Figure 4 shows the TEM micrographs of thin films of 1:1 alkoxide to water ratio processed at 400°C and 600°C for 60 minutes. At 300°C, the film overall was still amorphous, but by 400°C, the films were completely crystallized with crystallite size on the order of 30 nm. And as the temperature increased, the crystallites increased in size to about 125 nm and a porous network formed similar to that obtained at a high water to alkoxide ratios. At 600°C, Figure 4b shows the development of faceted particles. This is due to the domination of the low surface energy planes consistent with previous studies on the processing of  $\text{LiNbO}_3$  powders at 600°C [7].

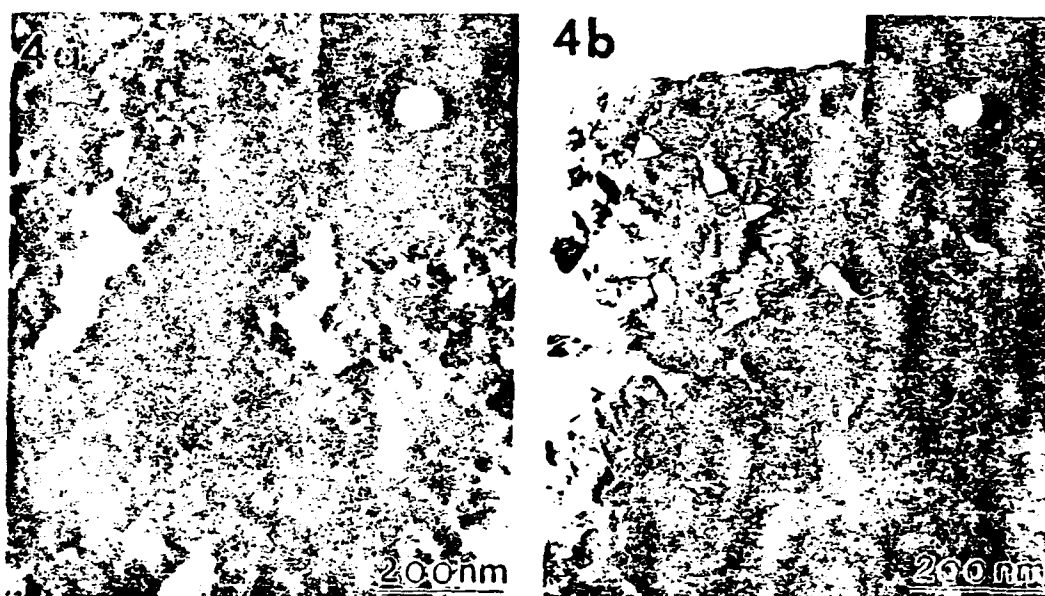


Figure 4: Film heat treated at (a) 400°C and (b) 600°C for 60 min. for 1:1 alkoxide/water ratio.

### Effect of soak time

The effect of soak time is shown in Figure 5 for selected samples with 1:1 alkoxide to water ratio held at 400°C. The film held for only 10 minutes appeared featureless and amorphous. After 30 minutes the film began to crystallize. As soak time increased, the size of the crystallites increased and a porous network forms (compare Figure 5a held for 60 min. and 5b held for 240 min). The grain size for the 240 min. sample is on the order of 150 nm which is similar to those obtained from films with a 1:2 alkoxide to water ratio heat treated for 1 hr. at 400°C (Fig. 3c), but the porosity is lower in the 1:1 sample held for 240 min.

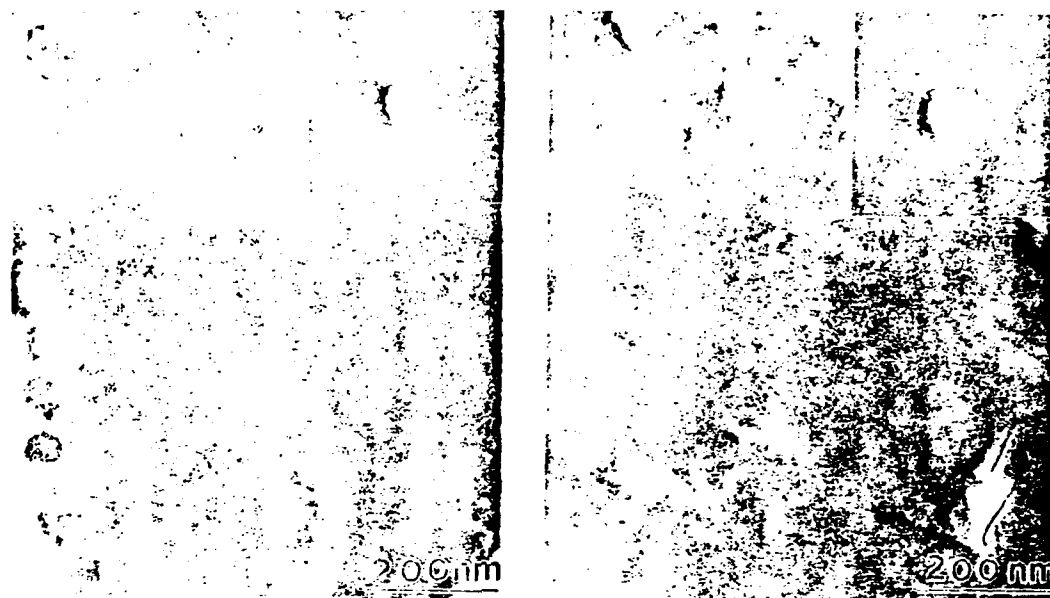


Figure 5: Film heat treated at 400°C for (a) 60 min. and (b) 240 min. for 1:1 alkoxide/water ratio.

#### Effect of substrate

Epitaxial film growth for lithium niobate was attempted using (0001) single crystal sapphire. Films were coated and treated at 400°C for 60 minutes for 1:1 alkoxide to water ratio. TEM examination of the film (1:1, 60 min. and 400°C) shows that the sapphire substrate yielded epitaxial growth over large areas. The SAD pattern in Figure 6 shows single crystal nature of the film and the zone axis is [0001]. The film were highly defective however, with significant strain, dislocations and twinning evident.

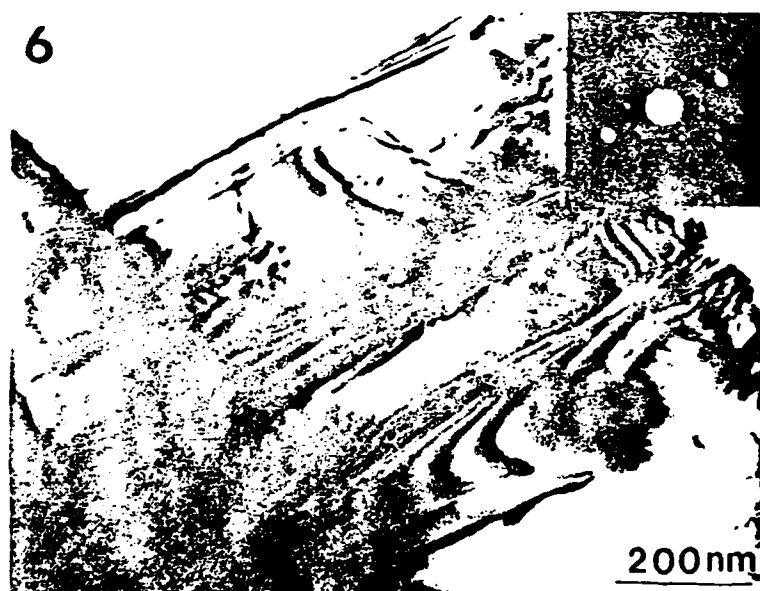


Figure 6:  $\text{LiNbO}_3$  film on single crystal sapphire (0001) substrate, heat treated at 400°C for 60 min. for 1:1 alkoxide/water ratio.

## CONCLUSION

The above results indicate that the film morphology for  $\text{LiNbO}_3$  can be tailored very explicitly by varying one or more of the following parameters: amount of water of hydrolysis, film treatment temperature, film treatment time. The higher the degree of hydrolysis, the larger the grain size and larger the pore size. Long times or high temperatures induced the formation of faceted large grains. Epitaxial film growth can be obtained on (0001) single crystal sapphire. More investigations are in process to achieve a defect-free epitaxial  $\text{LiNbO}_3$  film.

## ACKNOWLEDGMENTS

This work has been supported through a grant from the Air Force Office of Scientific Research under contract number 49620-89-C-0050.

## REFERENCES

1. S. Hirano and K. Kato, *J. Non-Cryst. Solids* **100**, 538 (1988).
2. N.P. Castings, F. Duboudin, and J. Ravez, *J. Mater. Res.* **3**, 557 (1988).
3. S. Hirano and K. Kato, *Advanced Ceramic Materials* **2**, 142 (1987).
4. D.P. Partlow and J. Gregg, *J. Mater. Res.* **2**, 595 (1987).
5. D.J. Eichorst and D.A. Payne, in *Better Ceramics Through Chemistry IV*, eds. B.J.J. Zelinski, C.J. Brinker, D.E. Clark, and D.R. Ulrich, (Mat. Res. Soc. Proc. **180**, Pittsburgh, PA, 1990) p. 669.
6. K. Nashimoto and M.J. Cima, *Mat. Lett.* **10**, 348 (1991).
7. V. Joshi, G.K. Goo, and M.L. McCartney, in *Synthesis and Processing of Ceramics: Scientific Issues*, eds. W.E. Rhine, T.M. Shaw, R.J. Gottschall, and Y. Chen (Mat. Res. Soc. Proc. **249**, Pittsburgh, PA, 1992), p.459.
8. M.G. Norton, S.R. Summerfelt, and C.B. Carter, *App. Phys. Lett.* **56**, 2246 (1990).